

THE NORMAL CO-ORDINATE ANALYSES,
VIBRATIONAL SPECTRA
AND THEORETICAL INFRARED INTENSITIES
OF SOME THIOCARBONYL HALIDE MOLECULES

THE NORMAL CO-ORDINATE ANALYSES,
VIBRATIONAL SPECTRA
AND THEORETICAL INFRARED INTENSITIES
OF SOME THIOCARBONYL HALIDE MOLECULES

A
THESIS
SUBMITTED TO
THE DEPARTMENT OF CHEMISTRY
IN PARTIAL FULFILMENT OF THE
REQUIREMENTS FOR THE DEGREE OF
MASTER OF SCIENCE
(CHEMISTRY)

JOHN L. BREMA B.Sc.

~~CONFIDENTIAL~~

BROCK UNIVERSITY
ST. CATHARINES, ONTARIO

1970

Abstract

TITLE: The normal co-ordinate analysis, vibrational spectra and theoretical infrared intensities of some thiocarbonyl halides.

AUTHOR: J. L. Brema

SUPERVISOR: Dr. D. C. Moule

NUMBER OF PAGES: 89

ABSTRACT: The vibrational assignment of the five-in-plane fundamental modes of CSClBr has been made on the basis of infrared gas phase and liquid Raman spectral analyses to supplement our earlier vibrational studies. Even though the one out-of-plane fundamental was not observed spectroscopically an attempt has been made to predict its frequency. The vibrational spectra contained impurity bands and the CSClBr assignment was made only after a thorough analysis of the impurities themselves.

A normal co-ordinate analysis calculation was performed assuming a Urey-Bradley force field. This calculation yielded the fundamental frequencies in good agreement with those observed after refinement of the originally transferred force constants. The theoretical frequencies are the eigenvalues of the secular equation and the calculation also gave the corresponding eigenvectors in the form of the very important $[L]$ matrix. The $[L]$ matrix is the transformation between internal co-ordinates and normal co-ordinates and it is essential for Franck-Condon calculations on electronically excited molecules and for infrared integrated band intensity studies.

Using a self-consistent molecular orbital calculation termed "complete neglect of differential overlap" (CNDO/2), theoretical values of equilibrium bond lengths and angles

were calcuted for a series of carbonyl and thiocarbonyl molecules. From these calculations valence force field force constants were also determined but with limited success. With the CNDO/2 method theoretical dipole moment derivatives with respect to symmetrized internal co-ordinates were calculated and the results should be useful in a correlation with experimentally determined values.

ACKNOWLEDGEMENTS

This work is but a mere reflection of the experience I have gained under the supervision of David Moule. I consider it a privilege to have worked closely with him for the past few years.

I wish to thank my immediate colleagues for their kind co-operation and friendship: C. T. Lin, P.D. Foo, D. G. McKinnon, C. R. Subramaniam and E. R. Farnworth. I am very grateful for the technical assistance so readily offered me by C. Misener, L. Westera, J. Neale, J. Vandenhoff, J. Ross and T. Biernacki. For their help in producing the photographs I wish to thank T. Squires and T. Russell.

I thank Dr. G. W. King's Spectroscopy group at McMaster University for obtaining many laser Raman spectra for me and also for the use of their computing facilities.

To my wife, Gay, thank you for your inspiration.

TABLE OF CONTENTS

	<u>Page</u>
Chapter 1	
Introduction	9
Chapter 2	
Theoretical	11
Chapter 3	
Preparation of CSClBr and Spectroscopic Techniques	16
Chapter 4	
The Vibrational Spectra (Infrared and Raman) of Thiocarbonyl Chlorobromide	19
Chapter 5	
Normal Co-ordinate Analysis	36
Chapter 6	
Infrared Intensities by the CNDO Method	62
Chapter 7	
Discussion	82

LIST OF FIGURES

		<u>Page</u>
Figure 4.1	Infrared spectrum of CSCl_2 (vapour)	20
Figure 4.2	Infrared spectrum of CSClBr (vapour)	21
Figure 4.3	Infrared spectrum of CSClBr (CS_2 solution)	25
Figure 4.4	Infrared spectrum of CSClBr (liquid)	26
Figure 4.5	Raman spectrum of CSClBr (liquid)	31
Figure 4.6	Raman spectrum of CSClBr (liquid) obtained with a higher resolution	32
Figure 4.7	Variation of out-of-plane frequency of carbonyl and thiocarbonyl halides with the square root of their molecular weights	35
Figure 6.1	Variation of CNDO/2 calculated total energy with bond length or angle for some C_{2v} symmetry molecules	71
Figure 7.1	CSClBr : Infrared vapour, CS_2 solution and liquid spectra; Raman liquid spectra	83

1911

1911

1	1911	1911
2	1911	1911
3	1911	1911
4	1911	1911
5	1911	1911
6	1911	1911
7	1911	1911
8	1911	1911
9	1911	1911
10	1911	1911
11	1911	1911
12	1911	1911
13	1911	1911
14	1911	1911
15	1911	1911
16	1911	1911
17	1911	1911
18	1911	1911
19	1911	1911
20	1911	1911
21	1911	1911
22	1911	1911
23	1911	1911
24	1911	1911
25	1911	1911
26	1911	1911
27	1911	1911
28	1911	1911
29	1911	1911
30	1911	1911
31	1911	1911
32	1911	1911
33	1911	1911
34	1911	1911
35	1911	1911
36	1911	1911
37	1911	1911
38	1911	1911
39	1911	1911
40	1911	1911
41	1911	1911
42	1911	1911
43	1911	1911
44	1911	1911
45	1911	1911
46	1911	1911
47	1911	1911
48	1911	1911
49	1911	1911
50	1911	1911
51	1911	1911
52	1911	1911
53	1911	1911
54	1911	1911
55	1911	1911
56	1911	1911
57	1911	1911
58	1911	1911
59	1911	1911
60	1911	1911
61	1911	1911
62	1911	1911
63	1911	1911
64	1911	1911
65	1911	1911
66	1911	1911
67	1911	1911
68	1911	1911
69	1911	1911
70	1911	1911
71	1911	1911
72	1911	1911
73	1911	1911
74	1911	1911
75	1911	1911
76	1911	1911
77	1911	1911
78	1911	1911
79	1911	1911
80	1911	1911
81	1911	1911
82	1911	1911
83	1911	1911
84	1911	1911
85	1911	1911
86	1911	1911
87	1911	1911
88	1911	1911
89	1911	1911
90	1911	1911
91	1911	1911
92	1911	1911
93	1911	1911
94	1911	1911
95	1911	1911
96	1911	1911
97	1911	1911
98	1911	1911
99	1911	1911
100	1911	1911

LIST OF TABLES

	<u>Page</u>
Table 4.1	23
CSClBr observed infrared frequencies, gas phase	
Table 4.2	27
CSClBr vibrational assignment, gas phase	
Table 4.3	27
CSClBr vibrational assignment, CS ₂ solution and liquid phases	
Table 4.4	33
CSClBr observed Raman frequencies, liquid	
Table 4.5	34
Laser Raman depolarization ratios, CSClBr liquid	
Table 5.1	56
Initial set of transferred Urey-Bradley force constants	
Table 5.2	58
[G] matrix elements for CSClBr	
Table 5.3	59
[Z] matrix elements for CSClBr	
Table 5.4	60
Urey-Bradley force constants for CSClBr	
Table 5.5	60
Calculated versus observed frequencies for CSClBr	
Table 5.6	61
[L] matrix elements for CSClBr	
Table 6.1	72
CNDO/2 equilibrium geometries	
Table 6.2	73
CNDO/2 quadratic valence force field force constants	
Table 6.3	79
CNDO/2 molecular dipole moment derivatives with respect to symmetrized internal coordinates	
Table 6.4	80
CNDO/2 output for an S ₁ type vibration for COCl ₂	
Table 7.1	84
Infrared and Raman assignments of CSClBr	
Table 7.2	86
Urey-Bradley in-plane force constants for CSF ₂ , CSClF, CSCl ₂ and CSClBr	

Chapter 1

Introduction

The first known studies of the vibrational fundamentals of thiocarbonyl chlorobromide were carried out by our spectroscopy group in 1969 (1). The work consisted of a partial normal co-ordinate analysis, the original synthesis of the compound and an assignment of the fundamentals based almost entirely on liquid and CS₂ solution phase studies of the infrared region of the spectrum. Due to unknown impurities of that time the gas phase analysis was of very little assistance in the vibrational assignment. The analysis of the ground state vibrations was undertaken as a necessary prelude to a detailed study of the electronic spectrum. In the past our group has achieved some success in the analysis of electronic transitions in related molecules (2,3,4,5). The present work is a continuation of the earlier work with its prime goal being the vibrational assignment based principally on gas phase spectra. Electronic spectra analyses require an accurate gas phase assignment of the fundamentals. It is a fact that liquid frequencies may be shifted from the corresponding gas phase values by undetermined amounts.

The original vibrational work was also hindered by the lack of a Raman study. Infrared and Raman methods of investigating molecules are most often complementary; the studies in one field frequently supplement or confirm the data derived from the other. One purpose of the present work was to seek a Raman analysis of the fundamentals. Raman spectra were obtained through the assistance of the Chemistry Department of McMaster University. The method proved to be a very helpful aid in the vibrational assignment of CSClBr.

A complete normal co-ordinate analysis was performed with the aid of an IBM-360 computer. It was found that the vibrational frequencies could be calculated most adequately with the use of a Urey-Bradley type potential function (6). The computer method was basically that as presented by Overend and Scherer in 1960 (7). By an iterative force constant refinement method we calculated the nine in-plane Urey-Bradley

force constants which we are able to correlate with similar calculations done by our group on CSF_2 , CSClF and CSCl_2 (2).

Work has recently started in this laboratory on the experimental measurement of integrated infrared band intensities. In conjunction with these studies we attempted the theoretical calculation of infrared intensities by the CNDO method, an approximate self-consistent molecular orbital theory. This method was first introduced by Segal and Klein in 1967 (8). Integrated band intensities are proportional to the change in the molecular dipole moment with respect to a normal co-ordinate, squared. Calculation of these dipole moment derivatives was performed on molecules of the type YXZ_2 ($\text{X} = \text{C}$, $\text{Y} = \text{O}, \text{S}$ and $\text{Z} = \text{H}, \text{F}, \text{Cl}$). The results of these calculations are very encouraging and should be very useful in the interpretation of forthcoming experimental data.

Chapter 2

vibrational Infrared Spectra and Intensities (9,10, 11)

The infrared absorption spectrum of a relatively heavy molecule consists of a series of bands, each of which results from a transition between a pair of vibrational levels associated with the ground electronic state. A typical absorption spectrum shows intense bands which are due to transitions from the ground state to states in which the normal vibrations are excited with single quanta (fundamentals), or lesser intensity bands due to transitions to higher vibrational states (overtones). There may also be weak intensity bands due to transitions originating on vibrationally excited states (combination bands).

An understanding of infrared intensities requires a close look at the mechanism by which light interacts with matter. In the presence of a radiation field there is a probability that a molecule will exchange energy with the field and appear in a quantum state other than its original one. If the molecule gains energy we observe absorption of radiation, if it loses energy, emission occurs. The quantum mechanical probability of a transition between upper state $\Psi_{v''}$ and lower state $\Psi_{v'}$, is

$$\left| \int \Psi_{v''}^* P \Psi_{v'} d\tau_v \right|^2 = \frac{8\pi^3}{3h^2} \langle v'' | P | v' \rangle^2 \rho(v_{v'',v'}) \quad (2.1)$$

if we assume that interactions between the vibrational, electronic and rotational motions are negligibly small, so that the integration can be carried out over the vibrational co-ordinate only. In equation (2.1)

$\langle v'' | P | v' \rangle$ is the quantum mechanical matrix element of the dipole moment, and $\rho(v_{v'',v'})$ is the density of the radiation of the particular frequency matching the quantum jump. The dipole moment P can be resolved into Cartesian components P_x , P_y and P_z , which transform under the symmetry operations of the point group the same as the corresponding translational motion components T_x , T_y or T_z . A transition can only occur between two vibrational states if the direct product for the group representations to which they belong transforms (or has a component that transforms) like

P_x , P_y or P_z , that is, like T_x , T_y or T_z respectively.

The probability that a molecule in an excited state will drop to a lower state is also given by (2.1) and if there are N'' molecules in the lower state and N' in the upper state, the net absorption probability is given by

$$\frac{8\pi}{3h^2} \langle v'' | P | v' \rangle^2 \rho(v_{v'',v'}) (N'' - N') \quad (2.2)$$

A small differential element of absorbing material of length dl and of unit cross-section will exchange energy with the radiation field according to (2.2). At each exchange the energy of the field will change by $(h\nu_{v'',v'})$ and the net loss of energy will be

$$-dI = \nu_{v'',v'} \frac{8\pi}{3h} \langle v'' | P | v' \rangle^2 \rho(v_{v'',v'}) (N'' - N') dl \quad (2.3)$$

The radiation flux and density are related by

$$I = c \rho \quad (2.4)$$

and equation (2.3) becomes

$$-d \ln I = \nu_{v'',v'} \frac{8\pi}{3hc} \langle v'' | P | v' \rangle^2 (N'' - N') dl \quad (2.5)$$

Upon integration (2.5) yields

$$\ln \frac{I_0}{I} = \nu_{v'',v'} \frac{8\pi}{3hc} \langle v'' | P | v' \rangle^2 (N'' - N') \quad (2.6)$$

At equilibrium the populations of the v' and v'' states follow the Boltzmann distribution expression and

$$(N'' - N') = n N_A^{-1} \{ \exp(-E_{v''}/kT) - \exp(-E_{v'}/kT) \} \quad (2.7)$$

where

$$A_v = \sum_i \exp(-E_i/kT) \quad (2.8)$$

and N is Avagadro's number and n the molar concentration.

The transition probabilities for all the rotational components also must be summed and this quantity compared with the total integrated intensity of the vibrational transition. The rotational components have the same vibrational matrix elements but slightly different frequencies so that it is more convenient to take the transition frequency of (2.6) over to the lefthand side of the equation. The summation over the rotational fine structure can be carried out exactly to yield

$$\Gamma_{v'',v'} = \frac{1}{nI} \int_{\text{band}} \ln \frac{I_0}{I} d \ln v = \frac{8\pi^3}{3hc} \langle v'' | P | v' \rangle^2 A_v^{-1} B \quad (2.9)$$

where

$$B = \{ \exp (-E_{v''}/kT) - \exp (-E_{v'}/kT) \} \quad (2.10)$$

Equation (2.9) is applicable to a fundamental transition, i.e. $v''=0$ to $v'=1$ and $A_v^{-1} B$ of (2.10) is close to unity so that a relatively simple expression is obtained

$$\Gamma_{v'',v'} = \frac{1}{nI} \int_{\text{band}} \ln \frac{I_0}{I} d \ln v = \frac{8\pi^3 N}{3hc} \langle 0 | P | 1 \rangle^2 \quad (2.11)$$

We assume that the vibrational motion is harmonic so that ψ_v can be factored into a product of harmonic oscillator functions $\psi(Q_i)$. The matrix element of the dipole moment is

$$\langle 0 | P | 1 \rangle = \int \psi_0^* (Q_i) P \psi_1 (Q_i) d\tau_v \quad (2.12)$$

The variation of P during vibration can be expressed as an expansion of each of its Cartesian components P_x , P_y and P_z in terms of normal coordinates. For P_x we write

$$P_x = (P_x)_0 + \sum_i \left(\frac{\partial P_x}{\partial Q_i} \right)_0 Q_i + \dots \quad (2.13)$$

where $(P_x)_0$ is the x component of the permanent dipole moment in the equilibrium position and higher terms in the expansion may be ignored for small displacements. The corresponding transition moment integral is

$$\int \Psi_{v''}^* P_x \Psi_v d\tau_v = (P_x)_0 \int \Psi_{v''}^* \Psi_v d\tau_v + \sum_i \left(\frac{\partial P_x}{\partial Q_i} \right)_0 \int \Psi_{v''}^* Q_i \Psi_v d\tau_v \quad (2.14)$$

The first integral on the right hand side vanishes as a result of the orthogonality of $\Psi_{v''}$ and Ψ_v , except in the trivial case where $v''=v$. If the eigenfunctions Ψ_v are written as a product of wave functions which depend on one normal co-ordinate

$$\Psi_v = \Psi(Q_1) \Psi(Q_2) \Psi(Q_3) \dots \Psi(Q_{3N-6}) \quad (2.15)$$

substitution of (2.15) in the i^{th} integral in the summation term gives

$$\begin{aligned} \int \Psi_{v''}^* Q_i \Psi_v d\tau_v &= \int \Psi_{v''}^* (Q_1) \Psi_v (Q_1) dQ_1 \int \Psi_{v''}^* (Q_2) \Psi_v (Q_2) dQ_2 \dots \\ &\dots \int \Psi_{v''}^* (Q_i) Q_i \Psi_v (Q_i) dQ_i \dots \end{aligned} \quad (2.16)$$

which vanishes unless $\Psi''(Q)=\Psi'(Q)$ for all normal co-ordinates except the i^{th} . If this condition is accepted all the integrals are unity except the one over Q_i and the i^{th} term in the summation of (2.14) becomes

$$\left(\frac{\partial P_x}{\partial Q_i} \right)_0 \int \Psi_{v''}^* (Q_i) Q_i \Psi_v (Q_i) dQ_i \quad (2.17)$$

This integral is the transition moment for two harmonic oscillator wave functions associated with one normal co-ordinate Q_i and is nonzero only if

$$\Delta v = \pm 1 \quad (2.18)$$

The matrix element of the dipole moment in (2.12) then becomes

$$\langle 0 | P | 1 \rangle = \left(\frac{\partial P_x}{\partial Q_i} \right)_0 \int \Psi_{v''}^* (Q_i) Q_i \Psi_{v'} (Q_i) dQ_i \quad (2.19)$$

The integral in (2.19) can be evaluated to yield

$$\langle 0 | P | 1 \rangle = \left(\frac{\partial P_x}{\partial Q_i} \right)_0 \left(\frac{\hbar}{8\pi^2 c \omega_i} \right)^{1/2} \quad (2.20)$$

where ω_i is the harmonic frequency of the i th mode. On substituting this result in (2.11) we obtain the explicit relationship between the integrated band intensity of a fundamental vibration and the derivative of the molecular dipole moment with respect to a normal co-ordinate in the form

$$\Gamma_i = \frac{N \pi}{3 c^2 \omega_i} \left(\frac{\partial P}{\partial Q_i} \right)^2 \quad (2.21)$$

where

$$\left(\frac{\partial P}{\partial Q_i} \right)^2 = \left(\frac{\partial P_x}{\partial Q_i} \right)^2 + \left(\frac{\partial P_y}{\partial Q_i} \right)^2 + \left(\frac{\partial P_z}{\partial Q_i} \right)^2$$

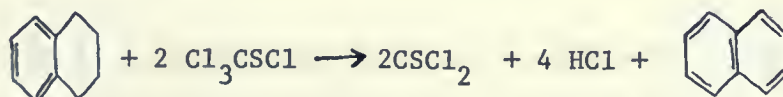
Chapter 3

Preparation of CSClBr and Spectroscopic Methods

3 (a) Experimental

The original synthesis of thiocarbonyl chlorobromide was achieved by the addition of anhydrous hydrogen bromide to thiophosgene under high pressure conditions. The reaction was carried out under vacuum in a Parr stainless steel bomb. The reaction product was very complicated and the best yield of CSClBr obtained by this method was 12.5% (1).

Another method has now been employed successfully to obtain an approximate 20% yield of CSClBr. This method was originally developed in our laboratory for the synthesis of CSClF (12). The present method consists of brominating thiophosgene with antimony tribromide in a non-aqueous solvent. The thiophosgene samples used were prepared at Brock University by Mr. I. D. Brindle. It was prepared by the slow addition of trichloromethanesulphenyl chloride to tetralin and heated at 200°C, the yield being about 80%.



The thiophosgene samples were handled very carefully. It is known that its vapour is a toxic substance which was used during WWI by the French and Austrians as a war gas under the name Lacrimite. The lethal concentration for 30 minutes exposure is reported to be 4000 mgm. per cubic metres of air (13).

In the present synthesis the SbBr_3 powder was dissolved in as little solvent as possible. The solvent used was tetrahydrothiophene -1,1-dioxide. Approximately 24 gms of SbBr_3 were reacted with 5 mls of liquid thiophosgene in order to theoretically achieve monobromination of the CSCl_2 . Under vacuum the SbBr_3 - solvent solution was slowly warmed to 50°C. The system was then pressurized with one atmosphere of dry nitrogen gas. The CSCl_2 liquid was added dropwise over an approximate period

period of one hour. During the addition of CSCl_2 drops of liquid SbCl_5 totalling 1 ml. were introduced into the reaction mixture. The mixture was allowed to stand for periods of from 1/2 to 3 days. The product mixture was then distilled into a sample vial at -197°C .

Purification of the product mixture proved to be very difficult. Trap to trap distillation with traps in series at -10° , -80° and -197°C eliminated the volatile components such as COCl_2 and SO_2 . Further purification attempts using fractional distillation methods with a cold finger at 0°C failed to remove the small quantities of CS_2 and CSCl_2 impurities. Mass spectra recorded on a Bendix Model 12 Time-of-Flight instrument revealed m/e parent peaks at 76 (CS_2), 114, 116 and 118 in the ratio of 9:6:1 (CSCl_2) and 158, 160 and 162 in the ratio of 3:4:1 (CSClBr). The impurities were readily separated by a Varian Model 700 preparative chromatograph using a 24 foot, 1/4" aluminum column packed with 30% Silicone Rubber (SE-30) on Chromosorb W. However, collection of the small (by volume) CSClBr fractions by Model 700's turntable mechanism was not successful.

3 (b) Infrared Spectra:

All infrared spectra were recorded on a Perkin - Elmer Model 225 grating infrared spectrophotometer over the range 4000 to 200 cm^{-1} . Over the range 4000 to 450 cm^{-1} the light dispersion element is a KBr prism and over the range 450 to 200 cm^{-1} a filter dispersion unit is automatically employed. The instrument is equipped with a dry air purging unit which reduces the amount of water vapour in the spectrophotometer to a negligible level. Over the region of the fundamental vibrations, namely 1200 to 200 cm^{-1} , the spectral slit widths ranged from 0.35 cm^{-1} to 1.55 cm^{-1} at the slit program setting of 1. The wave numbers of the CSClBr fundamentals were calibrated against those due to polystyrene film, atmospheric water vapour and carbon dioxide. The H_2O vapour bands at 1825.2 , 1616.7 , 506.95 and 374.54 cm^{-1} were constantly used as a calibration check along with the atmospheric CO_2 band at 671.34 cm^{-1} . The

resolution of the instrument was tested using a H_2O vapour doublet band at $473\dots472\text{ cm}^{-1}$ which has a separation of 0.5 cm^{-1} (14). When recording relatively high resolution spectra the abscissa axis was expanded by factors of 5 and 10, so as to accomodate 20 and 10% respectively of an individual range on the chart paper.

The liquid and CS_2 solution spectra of CSClBr were obtained by the methods reported in 1969 (1). The vapour phase spectra of the present work were obtained using 10 cm. pathlength cells fitted with KBr windows for the region 4000 to 500 cm^{-1} . The low frequency region, 500 to 200 cm^{-1} , required a 10 cm. gas cell fitted with polyethylene windows and a Perkin - Elmer 1 metre gas cell with CsI windows in which the beam path is folded several times by mirrors and remains geometrically unchanged upon leaving the cell. Uncertainties in the measurements of the observed band origins were estimated to be $\pm 2\text{ cm}^{-1}$ and $\pm 5\text{ cm}^{-1}$ in the vapour and liquid infrared respectively.

3(c) Raman Spectra

Raman spectra were obtained at McMaster University, Hamilton, Ontario. The liquid samples were contained in 1.8mm. O.D. (melting point) capillary tubes. The tubes were filled to a depth of approximately 1 cm. The radiation source was a He /Ne laser with incident exciting wavelength of 6328 \AA . The recording spectrograph was a Spex double monochromator model. The incident laser beam was plane polarized. With the use of a polarizer placed between the illuminator condensing lens and the spectrograph entrance slit polarization measurements were obtained. The polarizer was first placed at 0° (parallel) to the direction of the incident light vector and then at 90° (perpendicular) to the electric vector. Accurate intensity measurements are usually checked against CCl_4 intensity standards since the absolute intensities decrease non-linearly with increasing wavelength, an inherent characteristic of the photomultiplier tube in the system. Only relative linear intensities of the parallel and perpendicular components of the beam are required to obtain the depolarization ratio so that the absolute band intensities were not corrected. With this arrangement a Raman line is said to be completely depolarized if the ratio is three - quarters.

Chapter 4

The Vibrational Spectra (Infrared and Raman) of Thiocarbonyl Chlorobromide

The samples of this compound were contaminated with CSCl_2 and CS_2 and at times with SO_2 , COS , COCl_2 and COClBr so that absorption and emission resulting from fundamental vibrations of these molecules were present in the infrared and Raman spectra. Although an impurity free sample was never obtained a thorough analysis of the impurities enabled us to make an accurate assignment of the CSClBr fundamentals. The analysis was performed by means of Infrared spectroscopic techniques on gas, liquid and solution phase samples and by laser Raman spectroscopic techniques on liquid samples. The recorded spectra under these conditions are shown in this chapter as Figures 4.1 through 4.7 inclusive. These spectra generally cover the fundamentals region 1200 to 200 cm^{-1} . Table 4.1 lists the observed gas phase frequencies including fundamentals, overtones, combination and impurity bands. Table 4.2 shows the vibrational assignment based on gas phase spectra over the region 1200 to 200 cm^{-1} . Table 4.3 lists the liquid and solution spectra results and Table 4.4 gives the observed liquid laser Raman results.

The most serious impurity encountered was that of thiophosgene since its six fundamentals are very similar to those of thiocarbonyl chlorobromide. Thiocarbonyl chloride belongs to the C_{2v} point group and as such all of its six fundamentals should appear in both the infrared and Raman spectra.

Commercial thiophosgene, with a boiling point of approximately 70°C was purified to eliminate SO_2 and COCl_2 impurities. Its gas phase infrared and liquid phase Raman spectra were carefully studied in order to make an assignment for the ν_1 and ν_2 modes of thiocarbonyl chlorobromide. The gas phase infrared spectrum of pure CSCl_2 is shown in Figure 4.1 which, for the already mentioned reasons, is compared with Figure 4.2, the infrared gas phase spectrum of CSClBr .

Band contours which usually play an important role in determining the fundamental species of vibration for a molecule were generally not

Figure 4.1: Thiocarbonyl chloride (thiophosgene) infrared vapour spectrum over the region $1200 - 400 \text{ cm}^{-1}$. A 10 cm. pathlength cell with KBr windows was used and the gas was at a pressure of 1.00 cm Hg.

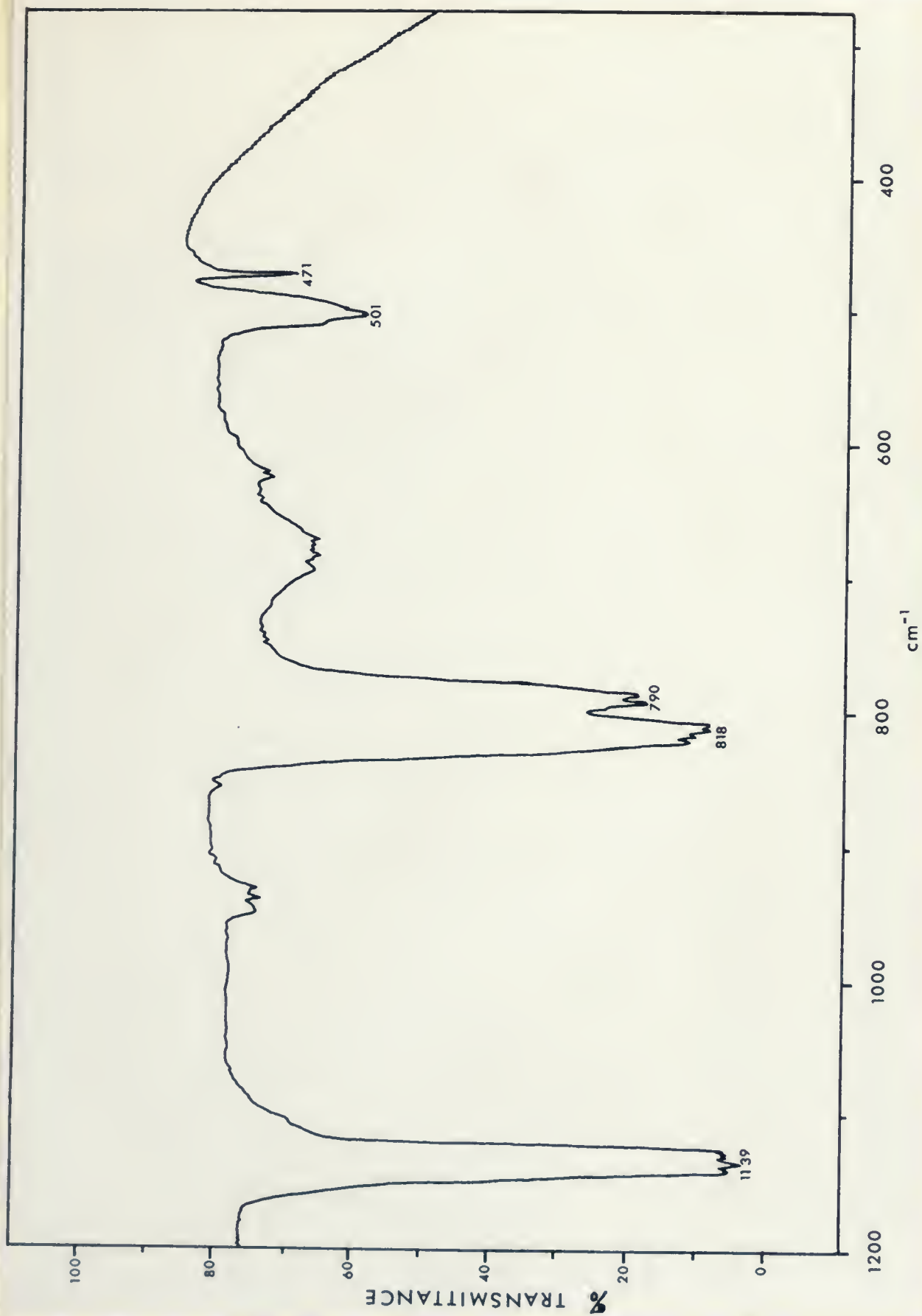
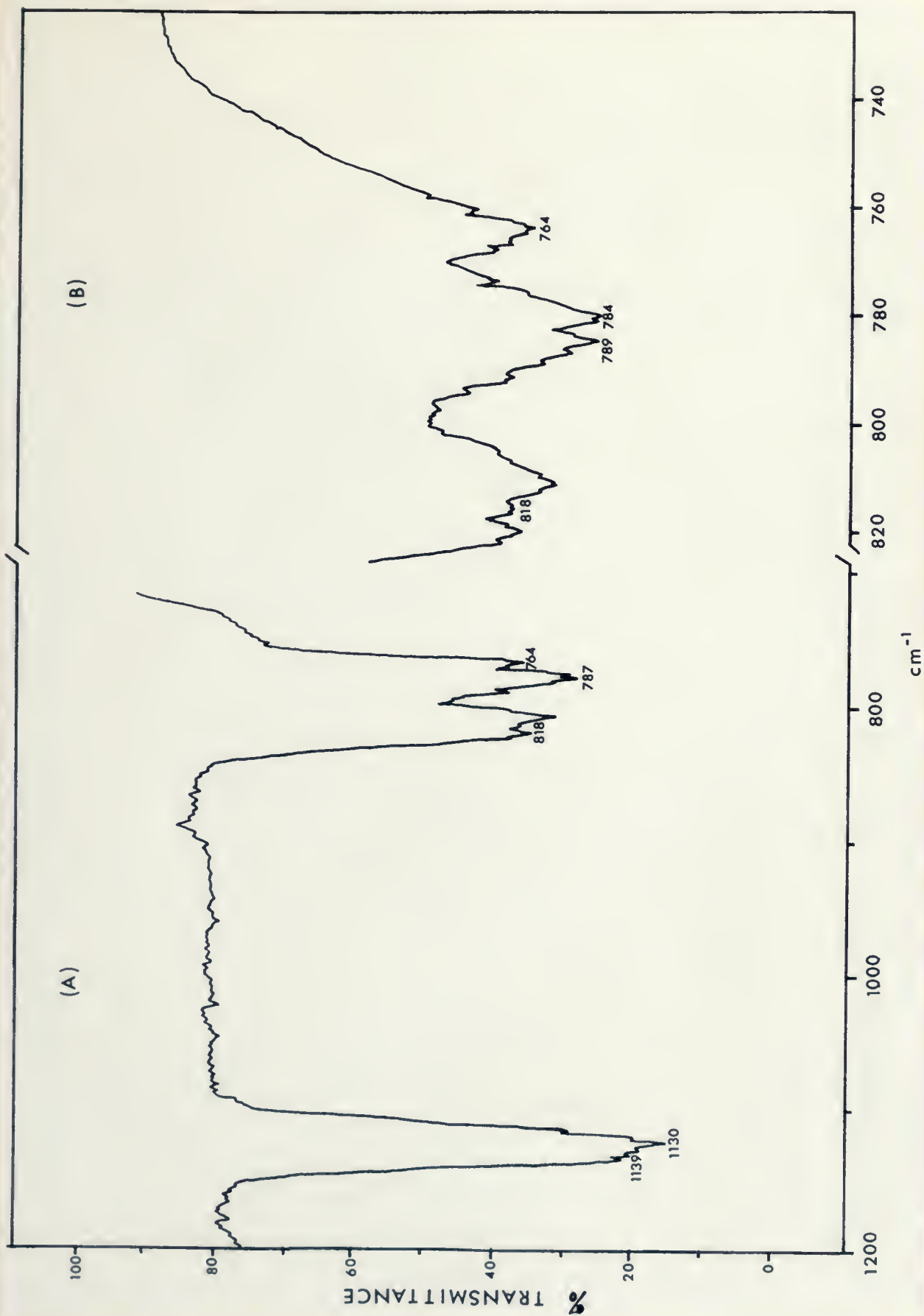


Figure 4.2: Thiocarbonyl chlorobromide Infrared vapour spectra at a pressure of 10 mm Hg taken in a 10 cm gas cell fitted with polyethylene windows. Section (a) shows fundamentals ν_1 and ν_2 over a normal wavelength scale. Section (b) shows the ν_2 fundamental over a blown up scale.



very useful in this study since CSClBr has only one a'' species of C-type contour. The other five fundamentals are of a' symmetry according to C_s point group restrictions, and as such, the dipole moment derivative change with respect to a normal co-ordinate for any fundamental may be in any direction in the xy molecular plane. This means that the vibration-rotation bands will have hybrid A,B type band contours.

The carbon-sulphur double bond stretching vibration in $CSCl_2$ is of A_1 symmetry and has a distinct type A band contour with its PQR structure maximum lying at 1139 cm^{-1} . and a PR separation of 14 cm^{-1} . This A-type band contour is lost in the spectrum shown of gas phase thiocarbonyl chlorobromide with $CSCl_2$ impurity as illustrated in Figure 4.2. In this case we observed from a blown up version of this spectrum a contour containing three maxima at 1139, 1134 and 1130 cm^{-1} . This pattern is consistent with the overlap of two type A contours corresponding to the C=S stretching modes of $CSCl_2$ and CSClBr. What seems to occur in the spectrum can be explained by rotational structure contour overlap. In effect, the thiophosgene C=S stretching mode has a PQR structure centred at 1139 cm^{-1} . In a similar manner the thiocarbonyl chlorobromide C=S stretching mode had a PQR structure centred at 1130 cm^{-1} . Because they fall so close together the R branch rotational contour due to the C=S stretch of $CSCl_2$ is super-imposed on the P branch rotational contour due to the C=S stretch of CSClBr giving rise to a spectroscopically artificial maximum at 1134 cm^{-1} . since the rotational bands are not resolved.

Further evidence for the existence of two superimposed fundamentals of these two molecules came from a measurement of band widths at half height which give a rough indication of the fundamental vibration. Spectra were recorded of 10.0 mm Hg. pressure gas samples of pure $CSCl_2$ and CSClBr using exactly the same I.R. gas cells and P.E. 225 instrument settings. The appropriate bands were measured to have band widths at half height such that the

Table 4.1

CSClBr, Vibrational Frequencies and Assignment
Infrared Spectrum (Gas Phase)

obs.(cm ⁻¹)	intensity	assignment	species	calc.(cm ⁻¹)
2266	m.w	CSCl ₂ impurity		
2249	m.w.	2ν ₁	a'	2260
2058	w.	COS impurity		
1606	m.w.	CSCl ₂ impurity		
1523	m.	CS ₂ impurity		
1514	m.	2ν ₂	a'	1526
1139	v.s.	CSCl ₂ impurity		
1130	v.s.	ν ₁	a'	1130
1021	w.	ν ₂ ⁺ ν ₄	a'	1022
869	w.	2ν ₃	a'	876
850	v.w.	COS impurity		
818	s.	CSCl ₂ impurity		
788	s.	CSCl ₂ impurity		
764	m.(sh)	ν ₂	a'	763
520	w.	COS impurity		
438	w.	ν ₃	a'	438
405	w.	CS ₂ impurity		
397	w.	CS ₂ impurity		
389	w.	CS ₂ impurity		
254	v.w.	ν ₄	a'	257

w= weak; s= strong; m= medium (intensity); v= very; sh= shoulder

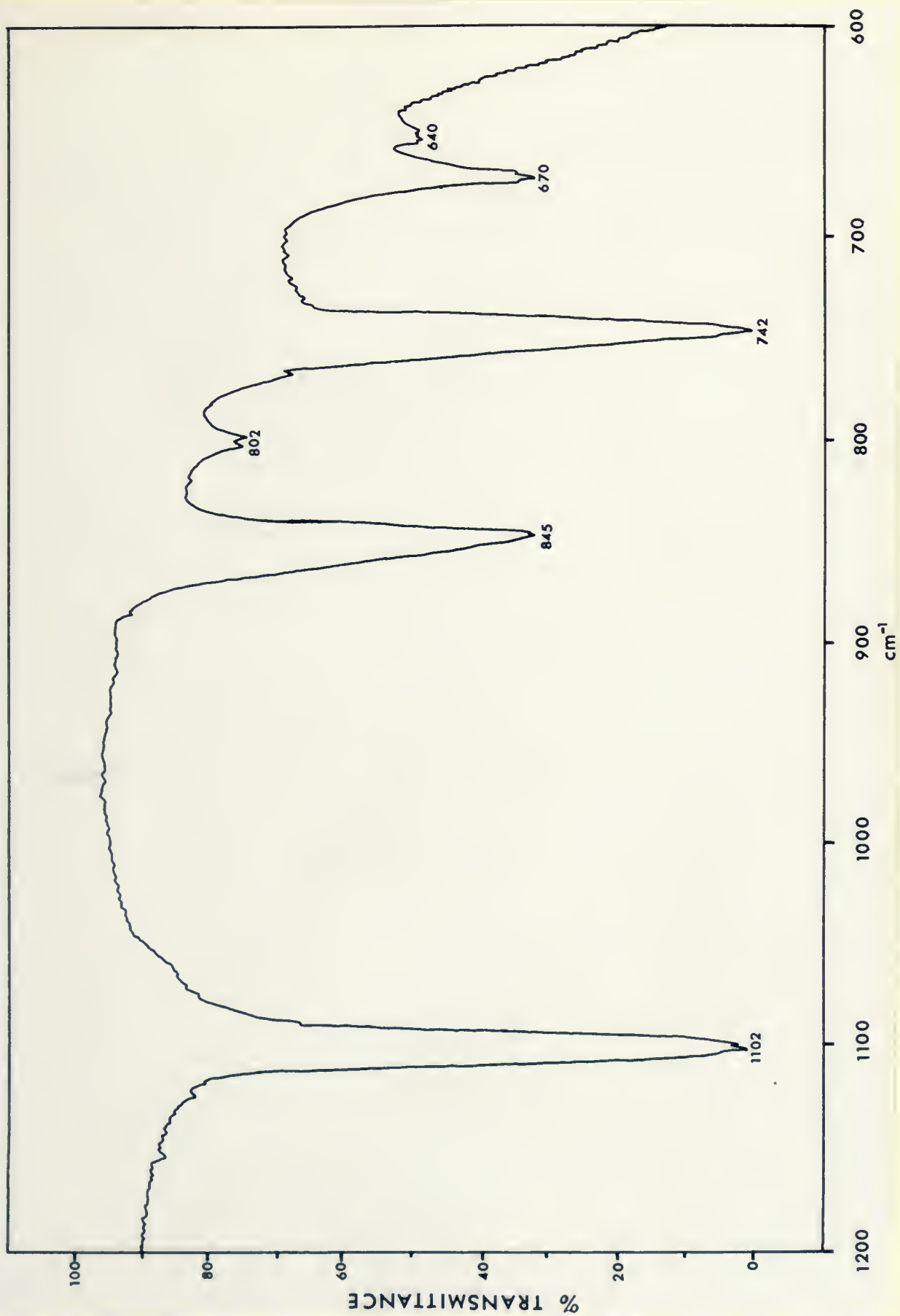
CSClBr sample was 35% wider corresponding to

	<u>CSCl₂</u>	<u>CSClBr</u>
$\Delta\nu_{\frac{1}{2}}$	31 cm ⁻¹	42 cm ⁻¹

On the basis of band contours and band widths at half height it is certain that the 1100 to 1150 cm⁻¹ region of spectrum as in Figure 4.2 was due to the 1139 cm⁻¹ ν_1 fundamental of CSCl₂ and the newly assigned 1130 cm⁻¹ ν_1 fundamental of CSClBr. Since rotational contours were not observed in the liquid Raman spectra the C = S stretching vibrations of CSClBr and CSCl₂ were not resolved. However, it is interesting to note that for pure CSCl₂ this fundamental always appeared at 1129 cm⁻¹ while for CSClBr samples a much broader band always appeared at 1125 cm⁻¹. Since the Raman samples were spectroscopically recorded at McMaster University the handling of the Spex instrument was not at our disposal and any conclusions drawn to explain this observed fact would be unjustified at this time.

In keeping with our method of pursuing a thorough analysis of impurities the 800 cm⁻¹ region of CSCl₂ as shown in Figure 4.1 was also looked at very carefully. Two peaks of importance are observed at 818 and 788 cm⁻¹. The 818 cm⁻¹ type B band has been assigned as the C - Cl₂ asymmetric stretch and the band at 788 cm⁻¹ the combination band of fundamentals at 500 cm⁻¹ and 292 cm⁻¹ (15). This band structure was consistently reproduced in spectra such as is shown in Figure 4.2 (A) for gas phase thiocarbonyl chlorobromide. However, for CSClBr spectra the shoulder band at 764 cm⁻¹ with no identifiable contour was evident. This band is better illustrated by Figure 4.2 (B) the blown up version of spectrum 4.2 (A). This band has often looked somewhat like a type A band but in any case it is assigned as the fundamental ν_2 for thiocarbonyl chlorobromide. Analogous to a similar vibration for CSCl₂

Figure 4.3: Infrared Spectrum of CSClBr in the liquid phase with CS_2 as the solvent over the region 1200 to 600 cm^{-1} . The cell used had Na Cl windows with a path length of 0.05mm.



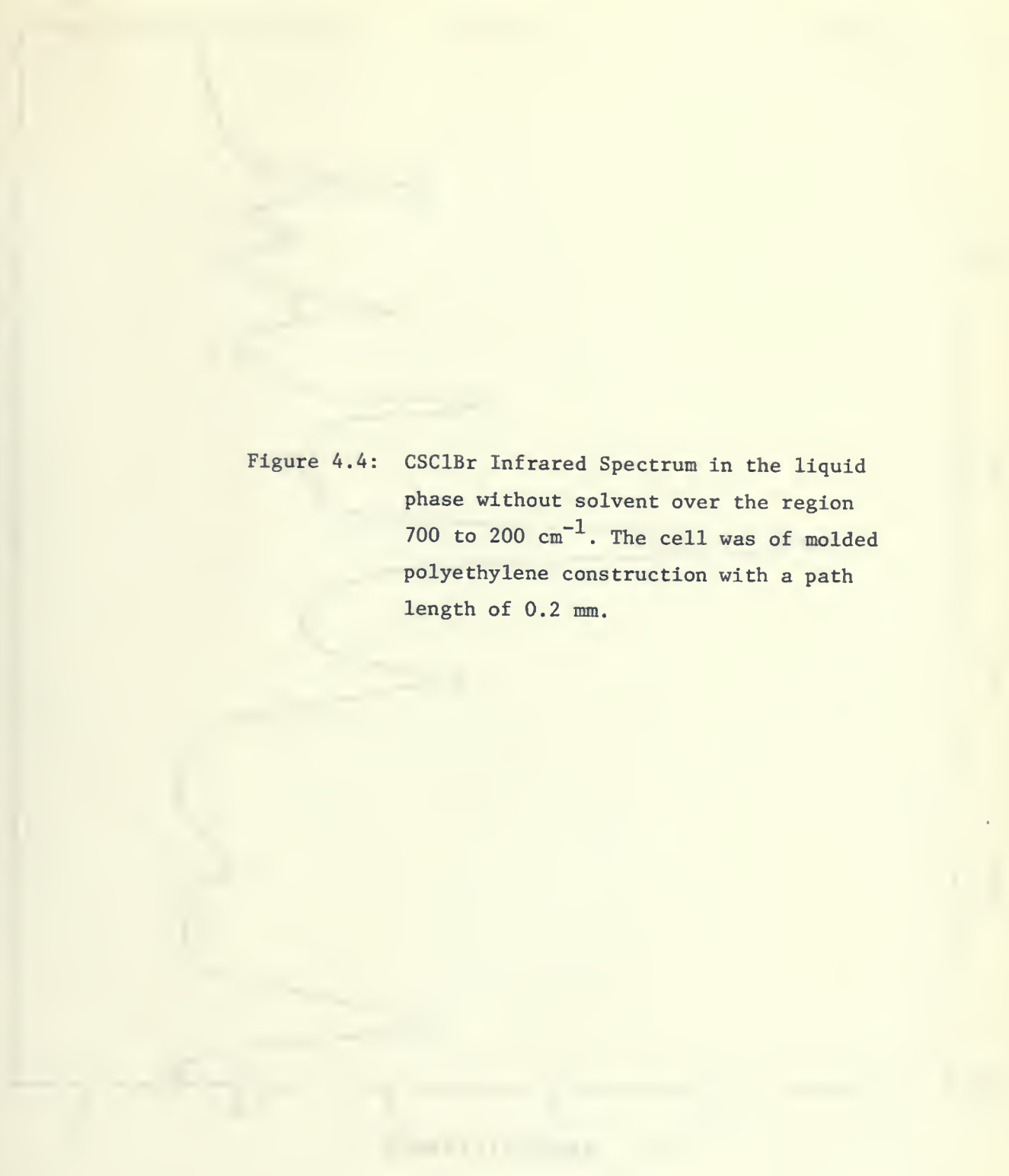
The image shows a very faint infrared spectrum plot. The x-axis represents wavenumber in cm⁻¹, and the y-axis represents transmittance. The spectrum shows several absorption bands, with a prominent one around 600 cm⁻¹ and another around 250 cm⁻¹. The plot is mostly illegible due to low contrast.

Figure 4.4: CSeBr Infrared Spectrum in the liquid phase without solvent over the region 700 to 200 cm^{-1} . The cell was of molded polyethylene construction with a path length of 0.2 mm.

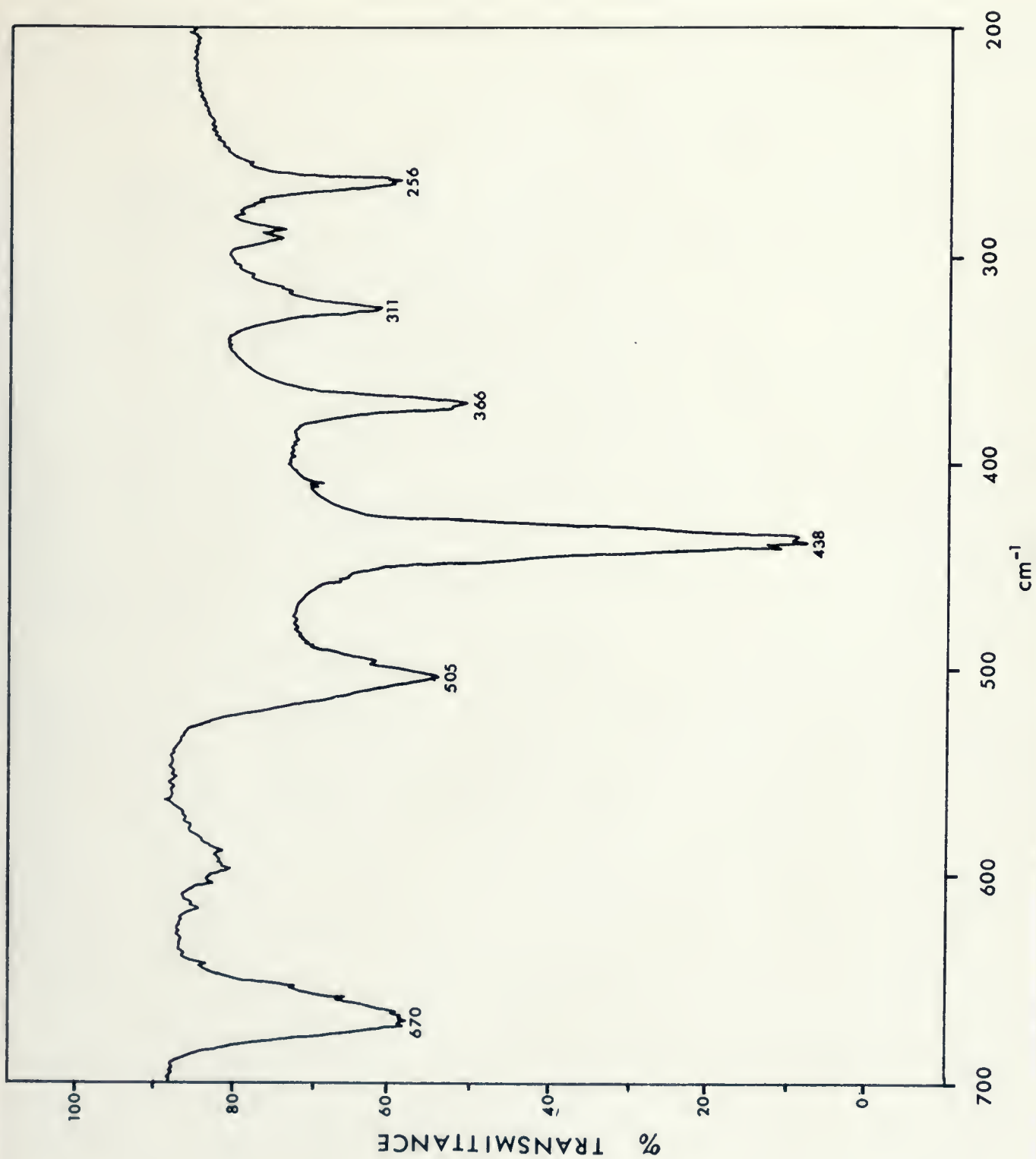


Table 4.2

Observed Infrared Frequencies for CSClBr			
Gas Phase			
Frequency (cm ⁻¹)	Intensity	Origin	Assignment
1139	s	CSCl ₂	ν ₁
1130	s	CSClBr	
818	s	CSCl ₂	
788	s	CSCl ₂	ν ₂
764	m (sh)	CSClBr	
438	w	CSClBr	
406	w	CS ₂	ν ₃
397	w	CS ₂	
389	w	CS ₂	

Table 4.3

Liquid and Solution Spectra			
Frequency (cm ⁻¹)	Intensity	Origin	Assignment
(a) 1104	s	CSCl ₂	ν ₁
1102	s	CSClBr	
845	s	CS ₂	
802	s	CSCl ₂	ν ₂
798	s	CSCl ₂ (CS ₂)	
742	m	CSClBr	
670	w	CS ₂	ν ₃
640	w	CS ₂	
(b) 505	m	CSCl ₂	
438	w	CSClBr	ν ₄
366	w	COBrCl	
316	w		
256	w	CSClBr	
(a) CS ₂	Solution spectra		
(b)	Pure liquid		

this vibration might be described as the ClCBr asymmetric stretch. In CSF_2 , CSClF and CSCl_2 , this type of vibration occurs at 1189, 1014 and 818 cm^{-1} respectively. By addition of bromine to CSCl_2 we expected this frequency to be less than 818 cm^{-1} , as we observe.

Figure 7.1 (A) illustrates the next fundamental to be assigned in the gas phase, the band at 438 cm^{-1} . This mode is assigned to be ν_3 for thiocarbonyl chlorobromide, the carbon chlorine stretching vibration. Its structure is not that of an A - type band. Following our work in 1969 it was thought that this band at 438 cm^{-1} was not ν_3 as we had assigned, but rather it was that of some COCl_2 impurity. For COCl_2 this band is assigned to ν_6 , a type B band of frequency 440 cm^{-1} (16). From a thorough study of the infrared spectrum of phosgene done in our laboratory we found this band to be of very weak intensity even at sample pressures near 760 mm.Hg. We concluded that this absorption band in COCl_2 would not be detected in CSClBr spectra of the type shown in Figure 4.3 at a pressure of 10 mm. Hg. This conclusion was recently found to be most justifiable after the integrated band intensity measurements obtained by Hopper, Russell and Overend for COF_2 , COCl_2 and COBr_2 (17). In crude figures their results revealed that if the most intense fundamental vibration of phosgene was arbitrarily given an integrated intensity value of 100% then the 440 cm^{-1} fundamental would have an integrated intensity value of 0.009%. With this piece of evidence it is certain that this band is not due to ν_6 of phosgene.

An interesting comparison arises between carbonyl and thiocarbonyl halides concerning the assignment of this C-Cl stretching mode at 438 cm^{-1} . From work done on carbonyl halides by Overend and Evans it is fact that for COCl_2 the CCl symmetric stretching mode ν_2 is assigned at 567 cm^{-1} (18). For COClBr this mode, termed ν_3 , is assigned at 517 cm^{-1} . This represents a frequency difference of 50 cm^{-1} . In the analogous thiocarbonyl halides ν_2 for CSCl_2 is assigned at 502 cm^{-1} (15). Our assignment for the ν_3 mode in CSClBr is 438 cm^{-1} , corresponding to a frequency difference of 64 cm^{-1} between CSCl_2 and CSClBr carbon chlorine stretching vibrations.

Also shown in Figure 7.1 (A) is the 400 cm^{-1} region of the gas phase infrared spectrum. From our own work done on the gas phase infrared of commercial carbon disulfide we found that the bands at 405, 397 and 389 cm^{-1} are those of the parallel type fundamental of CS_2 assigned ν_2 (19). We had expected the ν_6 out-of-plane fundamental of CSClBr to absorb in this region. However, as in the case of COClF , COClBr and CSClF this fundamental is of such weak intensity that it either didn't appear or was obscured by CS_2 impurity in the infrared. This out-of-plane mode should be quite intense in the electronic absorption spectrum of the visible region (20). The absolute assignment of this fundamental vibration cannot be made at this time but a prediction of its value can be made. In conjunction with the comparison drawn with the carbonyl halides in the previous paragraph we attempted to correlate the out-of-plane fundamentals of the carbonyl and thiocarbonyl halides. The resulting comparison is best exemplified by the graph shown in Figure 4.7. By drawing smooth curves through the appropriate points similar trends were obtained for both series of molecules. This graphical comparison is very similar to that employed by Shimizu and Shingu (21). They correlated vibrational frequencies for carbonyl halide out-of-plane deformation with electro-negativities and predicted a result for acetone. Since the carbonyl and thiocarbonyl halide molecules studied have the same basic geometry and vibrational type modes, it is not surprising that the curves of Figure 4.7 are so similar. On these grounds we predict ν_6 for CSClBr to have the frequency of 405 cm^{-1} .

The two remaining fundamental frequencies are the two in-plane vibrations ν_4 and ν_5 . These are assigned to be 256 and 222 cm^{-1} respectively. The ν_4 fundamental was observed only as a weak band at 256 cm^{-1} in the gas phase. The 222 cm^{-1} fundamental was never observed in the gas phase infrared. The ν_4 absorption band appeared in the pure liquid spectrum of Figure 4.4, as reported in 1969, and also in the liquid laser Raman spectrum. The ν_5 normal mode was observed only in the liquid Raman spectrum. These two fundamentals were expected to be of weak intensity and it proved very difficult to observe these bands in the gas phase infrared since the compound

is easily contaminated and has a small vapour pressure in vacuum at room temperature (approximately 1 cm. Hg). The ν_4 and ν_5 fundamentals can be described as the carbon bromine stretch and the bromine carbon chlorine angle bend respectively, although these descriptions are only approximate. It is somewhat coincidental that in a similar manner the corresponding ν_4 and ν_5 fundamentals in carbonyl chlorobromide were assigned as 372 and 240 cm^{-1} respectively by Overend and Evans on the spectral evidence that ν_4 was very weak in the gas phase IR and ν_5 was not observed at all (18). ν_5 was assigned solely on the basis of the band observed in the liquid Raman spectrum.

The pure liquid and CS_2 solution spectra shown in Figures 4.3 and 4.4 respectively are those obtained in the 1969 work. The analyses of these spectra remain basically the same as then and the assignments are listed in Table 4.3. The liquid and solution work proved to be very helpful.

Figure 4.5 illustrates the liquid laser Raman spectrum over the region 1200 to 200 cm^{-1} . Table 4.4 lists the observed frequencies, their intensities and assignments. The spectrum contains impurity bands due to the previously mentioned molecules CSCl_2 , CS_2 , and COClBr as well as another impurity, $(\text{CSCl}_2)_2$, thiophosgene dimer. Figure 4.6 shows the laser Raman spectrum resolved over the 800 cm^{-1} region. The relative intensity in this photograph is approximately twenty-five times that in the similar region of Figure 4.5. These spectra represent the condition under which the polarizer is parallel to the incident electric vector direction. The spectra shown in Figures 4.5 and 4.6 exhibit Raman shifts which are listed and assigned in Table 4.4. The five in-plane vibrations of CSClBr appear at 1125, 761, 437, 258 and 222 cm^{-1} respectively. Polarization measurements of these fundamentals showed them all to be polarized since the depolarization ratios were always less than 0.75 as shown in Table 4.5.

Figure 4.5: The liquid laser Raman spectrum of CSClBr over the range 1200 to 200 cm^{-1} . The excitation was achieved by a He/Ne laser source of 42 mW. power.

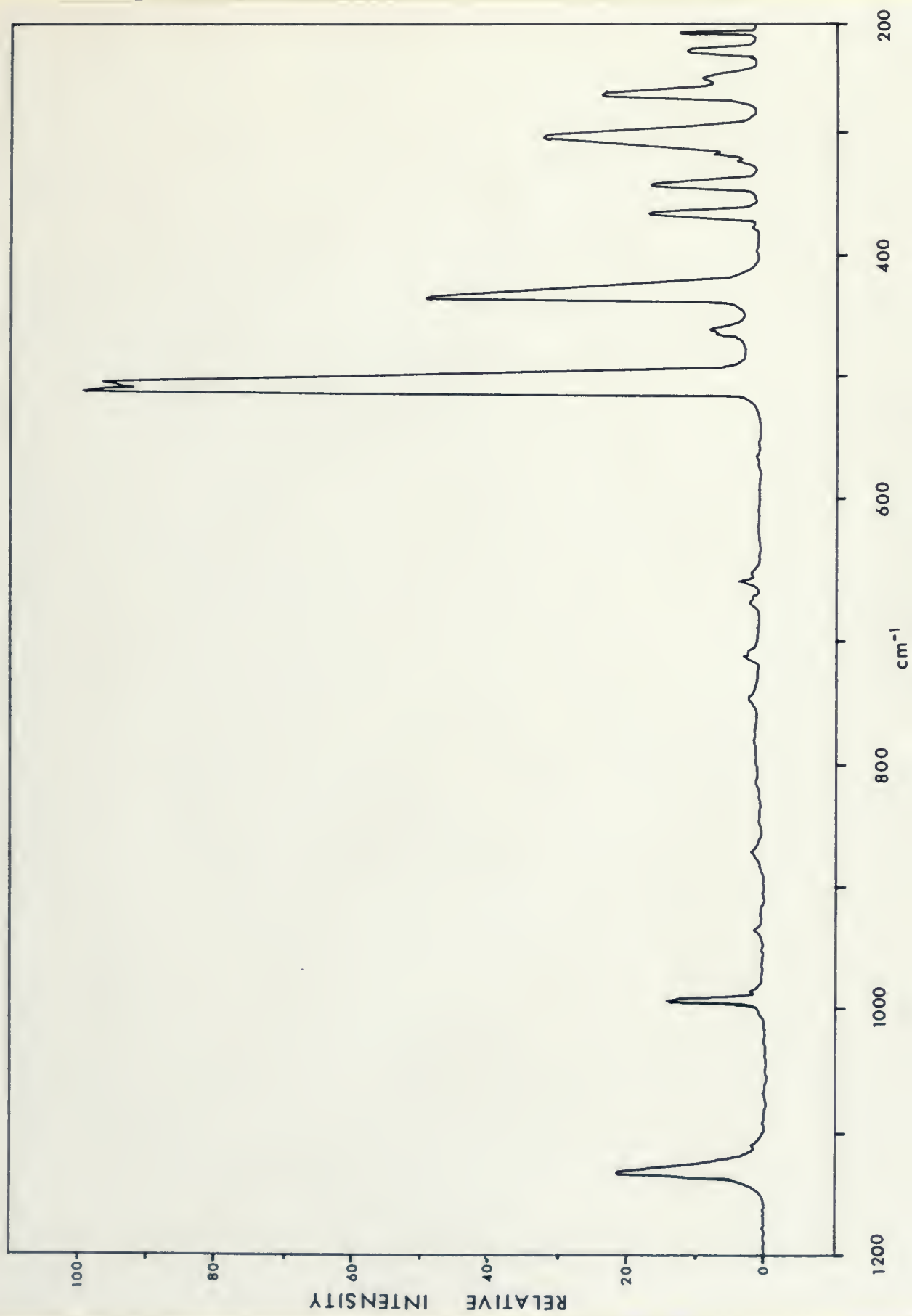


Figure 4.6: The 800 cm^{-1} region liquid CSClBr laser Raman spectrum under high resolution with the polarizer at 0° to the electric vector.

The smaller insert spectrum is the 800 cm^{-1} region laser Raman spectrum of liquid CSCl_2 as obtained by Frenzel and Blick. These workers note two CSCl_2 bands, two $(\text{CSCl}_2)_2$ bands and a trimer shoulder at 834 cm^{-1} in this region.

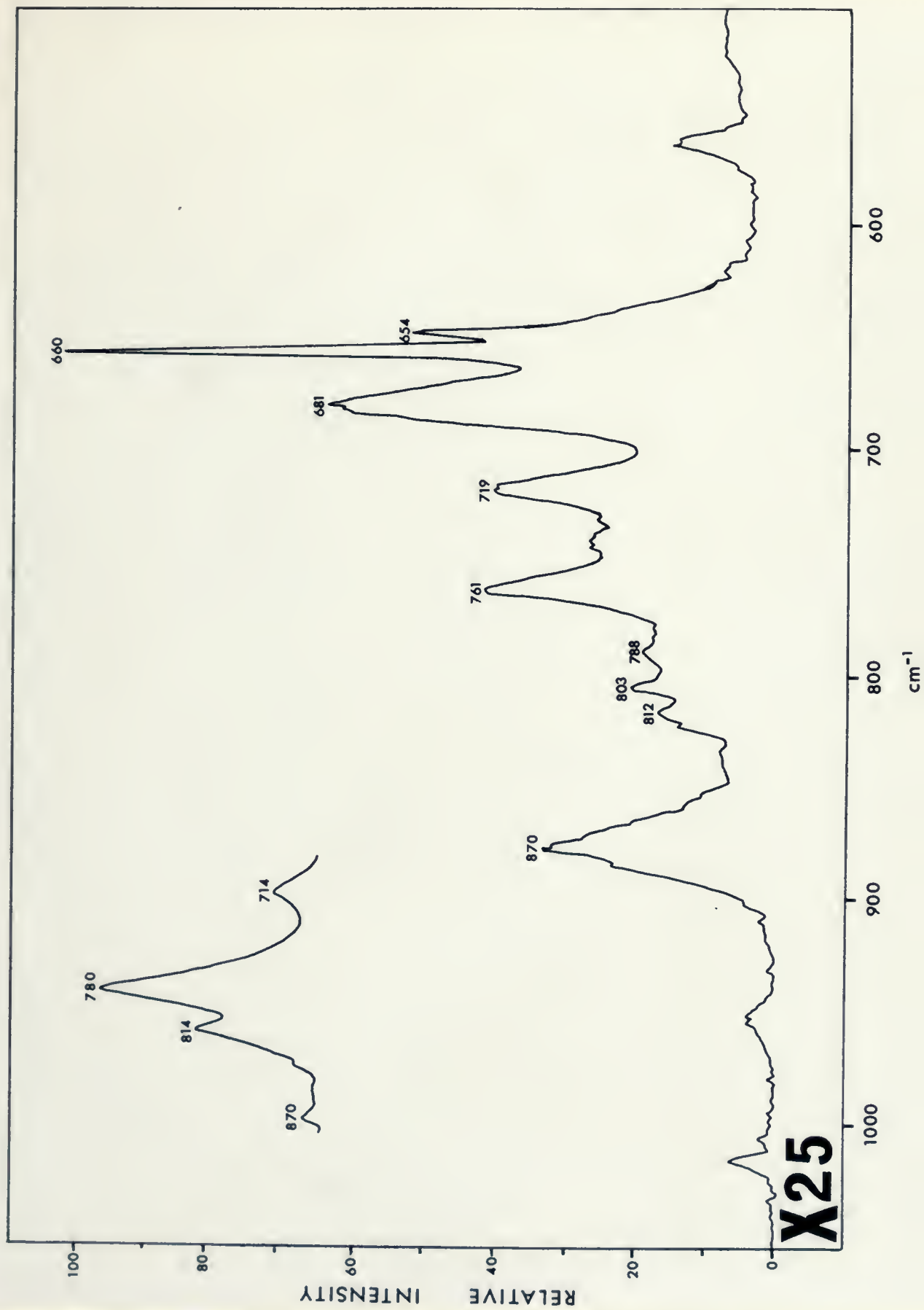


Table 4.4

CSClBr, Vibrational Frequencies and Assignment Laser Raman Spectra (Liquid Phase)			
Frequency (cm^{-1})	Intensity	Assignment	Species
1125	s	CSCl ₂ & CSClBr	a'
871	vw	(CSCl ₂) ₂ impurity	
812	vw	CSCl ₂ impurity	
804	vw	CS ₂ impurity	
788	vw	CSCl ₂ impurity	
761	vw	CSClBr	a'
743	vw	(CSCl ₂) ₂ impurity	
720	vw	(CSCl ₂) ₂ impurity	
660	vw	CS ₂ impurity	
654	vw	CS ₂ impurity	
505	s	COC1Br impurity	
501	s	CSCl ₂ impurity	
460	w		
437	m	CSClBr	a'
370	w	COC1Br	
344	w		
301	m	CSCl ₂ impurity	
258	mw	CSClBr	a'
241	w	COC1Br	
222	w	CSClBr	a'
202	w	(CSCl ₂) ₂ impurity	
178	w		

Table 4.5

Fundamental	Raman Frequency (cm^{-1})	Depolarization Ratio ρ
ν_1	1125	0.17
ν_2	761	0.67
ν_3	437	0.12
ν_4	258	0.46
ν_5	222	0.50

All of the impurity bands listed in Table 4.4 were assigned except for the bands at 460, 344 and 178 cm^{-1} . COCl_2 did not prove to be much of a problem in the Raman (22). The out-of-plane fundamental, ν_6 , did not show up in the Raman spectrum but this has also been the case for other thiocarbonyl halide liquid Raman studies to date (12,23). Three of the impurity bands in the liquid Raman have been assigned as those due to thiophosgene dimer according to the recent work of Frenzel et al. (23). These assignments are reasonable since the dimer can be readily prepared by irradiation with a laser beam, the same condition under which our Raman samples were excited.

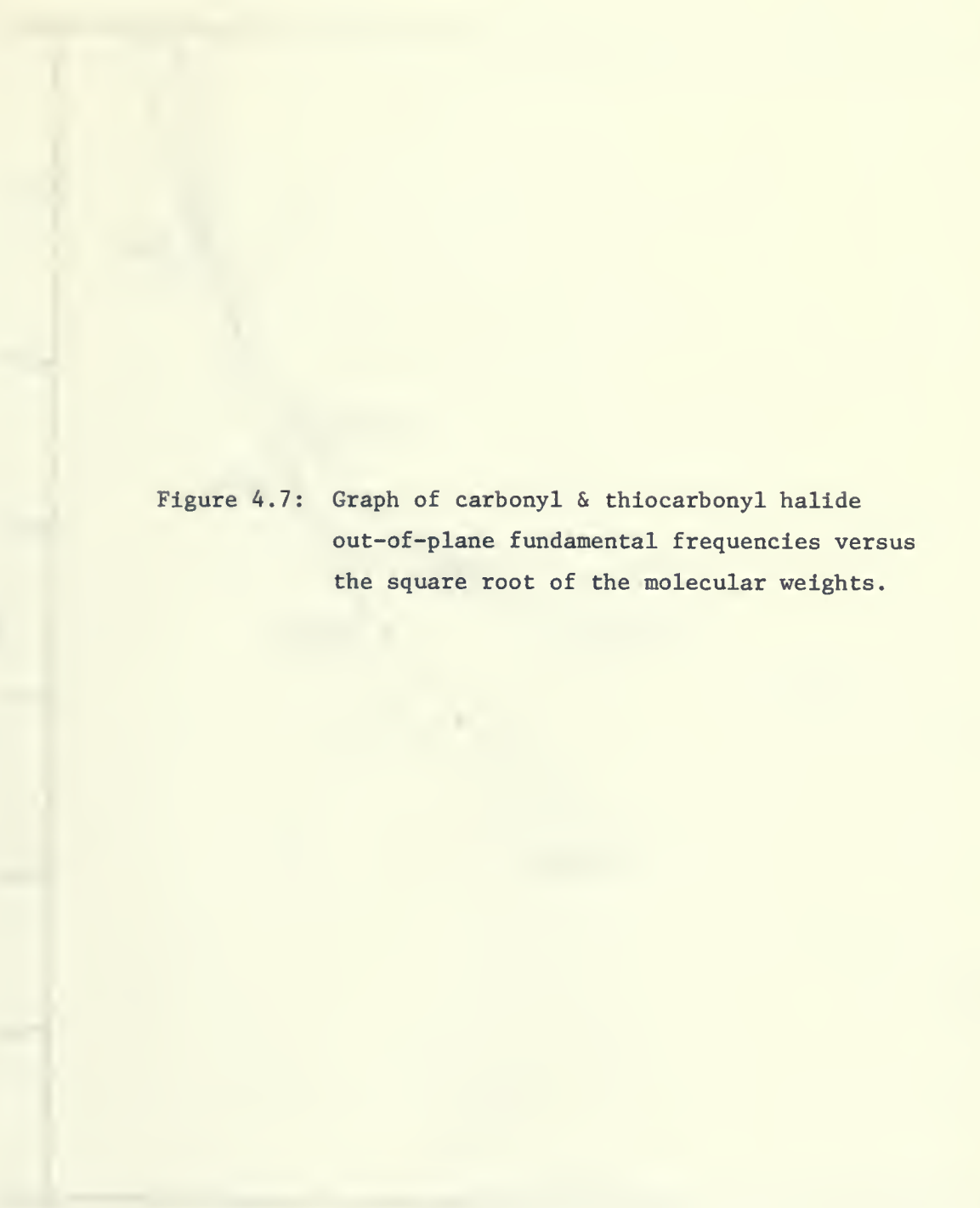
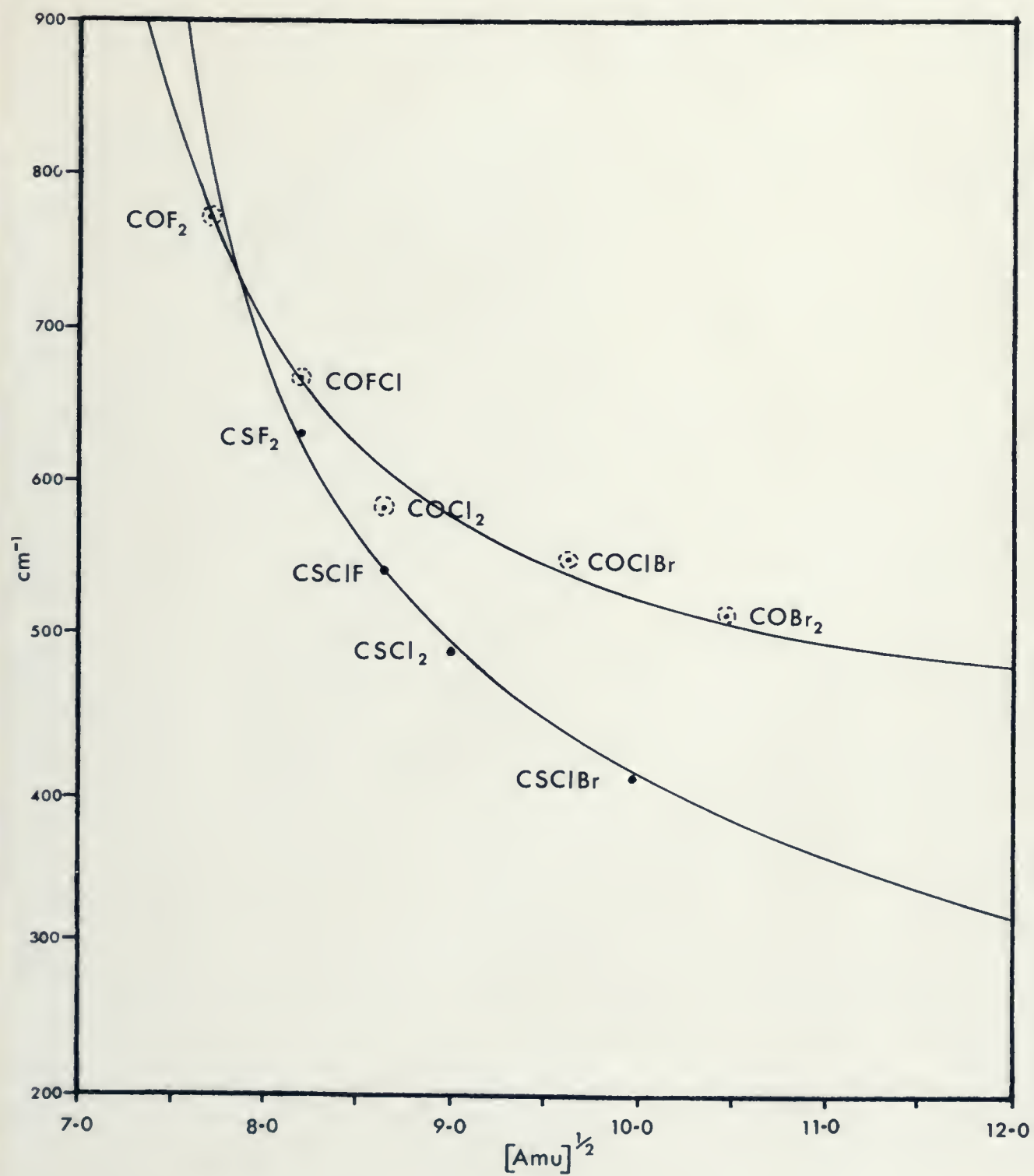


Figure 4.7: Graph of carbonyl & thiocarbonyl halide out-of-plane fundamental frequencies versus the square root of the molecular weights.



Chapter 5

Normal Co-ordinate Analysis

The model for a molecule that we employ in the analysis of vibrations is that of N point masses, representing the nuclei, which are elastically coupled together. In the simple harmonic oscillator approximation the displacement of the nuclei from their equilibrium positions is relatively small compared to the bond lengths and the distances between non-bonded atoms of the model. The elastic coupling between masses, regardless of its nature, assumes the presence of restoring forces which return the displaced nuclei to their equilibrium locations. The restoring forces are described by the mathematical potential energy function for the system and these restoring forces are independent of the electronic motion.

A stable molecule has three translational and three rotational degrees of freedom and the remainder of the $3N-6$ total degrees of freedom are vibrational degrees of freedom. A linear molecule has $3N-5$ total degrees of freedom of which only two are rotational degrees of freedom. It is usually convenient to solve the equations of motion for $3N$ co-ordinates and then remove the rotational and translational motions. This is achieved by employing "molecule-fixed" displacement vectors for each nucleus so that the center of mass of the system does not translate and the net angular momentum is zero.

The writing of the classical equations of motion is simplified by using $\xi_1, \xi_2, \xi_3, \xi_4, \dots, \xi_{3N}$ as the symbols for the Cartesian displacement co-ordinates $x_1, y_1, z_1, \dots, x_N, y_N, z_N$. When the nuclei are displaced from their equilibrium positions the restoring forces can be described by those obeying Newton's laws:

$$f_i = m_i \ddot{\xi}_i \quad (i=1,2,3,\dots,3N) \quad (5.1)$$

The $3N$ Newtonian equations are complicated to solve in terms of Cartesian co-ordinates so that the equations of motion are often written in the alternative Lagrangian form which is independent of any particular co-ordinate system. The potential field is then a function of the generalized co-ordinates q_i

$$V(q_1, q_2, q_3, q_4, \dots, q_{3N}) \quad (5.2)$$

The equivalent Lagrangian equations of motion can then be written in terms of the generalized co-ordinates which are compatible with any particular co-ordinate system chosen

$$\frac{d}{dt} \cdot \frac{\partial L}{\partial \dot{q}_i} - \frac{\partial L}{\partial q_i} = 0 \quad (i=1,2,3,\dots,3N) \quad (5.3)$$

where L , the Lagrangian function for the molecule, is the excess of kinetic energy over potential energy

$$L = T - V \quad (5.4)$$

If the general co-ordinates q_i are Cartesian co-ordinates the kinetic energy is

$$T = \frac{1}{2} m_1 \dot{\xi}_1^2 + \frac{1}{2} m_2 \dot{\xi}_2^2 + \frac{1}{2} m_3 \dot{\xi}_3^2 + \dots + \frac{1}{2} m_{3N} \dot{\xi}_{3N}^2 \quad (5.5)$$

or

$$2T = \sum_{i=1}^{3N} m_i \dot{\xi}_i^2 \quad (5.6)$$

If the general co-ordinates q_i are mass-weighted Cartesian co-ordinates the kinetic energy is

$$2T = \sum_{i=1}^{3N} \dot{\eta}_i^2 \quad (5.7)$$

where

$$\eta_i = \sqrt{m_i} \xi_i \quad (5.8)$$

The potential energy V can be expressed as a Taylor series about the equilibrium positions of the nuclei

$$V = V_0 + \sum_{i=1}^{3N} \left(\frac{\partial V}{\partial \xi_i} \right)_0 \xi_i + \frac{1}{2} \sum_{j,i=1}^{3N} \left(\frac{\partial^2 V}{\partial \xi_i \partial \xi_j} \right)_0 \xi_i \xi_j + \dots \quad (5.9)$$

Terms higher in order than the quadratic one can be neglected since the simple harmonic oscillator approximation has been assumed. The potential energy can always be measured relative to the value in the equilibrium position so that $V_0 = 0$. With all nuclei situated such that their positions represent the equilibrium positions, a potential energy minimum is achieved making the first order derivatives also equal to zero. Hence,

$$2V = \sum_{j,i=1}^{3N} \left(\frac{\partial^2 V}{\partial \xi_i \partial \xi_j} \right)_0 \xi_i \xi_j \quad (5.10)$$

Since all the second order derivatives are constant the potential expression is given by

$$2V = \sum_{j,i=1}^{3N} b'_{ij} \eta_i \eta_j \quad (5.11)$$

where

$$b'_{ij} = \left(\frac{\partial^2 V}{\partial \xi_i \partial \xi_j} \right)_0 = b'_{ji} = \text{constant} \quad (5.12)$$

In terms of mass-weighted Cartesian co-ordinates

$$2V = \sum_{j,i=1}^{3N} b_{ij} \eta_i \eta_j \quad (5.13)$$

Equations (5.7) and (5.13) give T and V in terms of mass-weighted Cartesian co-ordinates and the Lagrangian equation of motion (5.3) can be written

$$\frac{d}{dt} \cdot \frac{\partial L}{\partial \dot{\eta}_i} - \frac{\partial L}{\partial \eta_i} = 0 \quad (5.14)$$

which reduces to

$$\ddot{\eta}_i + \sum_{j=1}^{3N} b_{ij} \eta_j = 0 \quad (5.15)$$

Equations of the type (5.15) are known to be those of the harmonic oscillator which have solutions of the form

$$\eta_i = \eta_i^0 \sin \left(t \lambda^{\frac{1}{2}} + \delta \right) \quad (5.16)$$

where η_i^0 , λ and δ are constants. Substitution of (5.16) into (5.15) yields

$$\sum_j b_{ij} \eta_j^0 - \lambda \eta_i^0 = 0 \quad (i=1,2,3,\dots,3N) \quad (5.17)$$

which can be rearranged as

$$\sum_{i \neq j} b_{ij} \eta_j^0 + b_{ii} \eta_i^0 - \lambda \eta_i^0 = 0$$

or

$$\sum_{i \neq j} b_{ij} \eta_j^0 + (b_{ii} - \lambda) \eta_i^0 = 0 \quad (5.18)$$

These $3N$ simultaneous equations (5.18) are only non-trivial if the matrix array of η_i^0 coefficients

$$\begin{bmatrix} b_{11} - \lambda & b_{12} & \dots & b_{1,3N} \\ b_{21} & b_{22} - \lambda & \dots & b_{2,3N} \\ \vdots & \vdots & \ddots & \vdots \\ b_{3N,1} & b_{3N,2} & \dots & b_{3N,3N} - \lambda \end{bmatrix} = 0 \quad (5.19)$$

or in the secular form

$$| b_{ij} - \lambda \delta_{ij} | = 0 \quad (5.20)$$

where

$$\begin{aligned} \delta_{ij} &= 0 & \text{for } i \neq j \\ \delta_{ij} &= 1 & \text{for } i = j \end{aligned}$$

Equation (5.20) has $3N$ roots; $\lambda_1, \lambda_2, \lambda_3, \dots, \lambda_{3N}$. Each λ_k greater than zero represents a harmonic oscillator mode of the atoms according to

$$\eta_i = \eta_i^0 \sin (t \lambda_k^{1/2} + \delta) \quad (5.16)$$

of frequency ν_k where

$$\lambda_k = 4\pi^2 c^2 v_k^2 \quad (\text{cm}^{-1}) \quad (5.21)$$

and

$$v_k = \frac{1}{2\pi} \sqrt{\frac{k_k}{\mu}} \quad (5.22)$$

where k_k is the appropriate restoring force constant and μ is the reduced mass of the system of point masses. The values v_k are the fundamental frequencies of vibration. If n of the v_k 's are of the same value an n -fold degeneracy occurs. Six of the roots will have the value $\lambda = 0$. These represent translational and rotational motions of the molecule with zero frequency of vibration. Roots with λ_k less than zero do not occur for molecules with chemically stable equilibrium configurations.

Assuming a non-degenerate set of λ_k 's, substitution of (5.16) into (5.17) yields

$$\begin{aligned} b_{11}\eta_{1k}^0 + b_{12}\eta_{2k}^0 + b_{13}\eta_{3k}^0 + \dots + b_{1,3N}\eta_{3N,k}^0 - \eta_{1k}^0 \lambda_k &= 0 \\ b_{21}\eta_{1k}^0 + b_{22}\eta_{2k}^0 + b_{23}\eta_{3k}^0 + \dots + b_{2,3N}\eta_{3N,k}^0 - \eta_{2k}^0 \lambda_k &= 0 \\ \cdot &\cdot \\ \cdot &\cdot \\ \cdot &\cdot \\ \cdot &\cdot \\ b_{3N,1}\eta_{1k}^0 + b_{3N,2}\eta_{2k}^0 + b_{3N,3}\eta_{3k}^0 + \dots + b_{3N,3N}\eta_{3N,k}^0 - \eta_{3N,k}^0 \lambda_k &= 0 \end{aligned} \quad (5.23)$$

Since there are $3N$ equations and $3N$ unknowns one extra equation is required to determine the absolute values of η_{ik}^0 . Solving the set of equations (5.23) gives the ratios

$$\eta_{1k}^0 : \eta_{2k}^0 : \eta_{3k}^0 : \dots : \eta_{3N,k}^0 \quad (5.24)$$

for each λ_k . A new set of coefficients l_{ik} are formulated in the same ratio as the η_{ik}^0 's but which are normalized according to

$$\sum_i l_{ik}^2 = 1 \quad (5.25)$$

where

$$\eta_{ik}^0 = K_k l_{ik}$$

The coefficients l_{ik} can be written in the form analogous to equation

(5.23) and the values l_{ik} and K_k determined for each root λ_k . The l_{ik} 's are also written as a set of column vectors

$$\begin{bmatrix} l_{11} \\ l_{21} \\ \cdot \\ \cdot \\ \cdot \\ l_{3N,1} \end{bmatrix} \begin{bmatrix} l_{12} \\ l_{22} \\ \cdot \\ \cdot \\ \cdot \\ l_{3N,2} \end{bmatrix} \begin{bmatrix} l_{13} \\ l_{23} \\ \cdot \\ \cdot \\ \cdot \\ l_{3N,3} \end{bmatrix} \dots \dots \dots \begin{bmatrix} l_{1,3N} \\ l_{2,3N} \\ \cdot \\ \cdot \\ \cdot \\ l_{3N,3N} \end{bmatrix} \quad (5.26)$$

Each l_{ik} of each column vector is proportional to the amplitude of the appropriate η_i^0 and therefore the appropriate ξ_i^0 . The individual sets of column vector coefficients can be used as vectors attached to the nuclei showing the displacements undergone by the nuclei during each normal vibration.

With the advent of computer aided techniques during the past dozen years it has become standard procedure to describe and solve the mathematical molecular vibration problem in terms of matrix algebra. The kinetic energy becomes

$$2T = \sum_{i=1}^{3N} \dot{\eta}_i^2 = [\dot{\eta}]^t [\dot{\eta}] \quad (5.27)$$

and the potential energy is

$$2V = \sum_{j,i=1}^{3N} b_{ij} \eta_i \eta_j = [\eta]^t [B] [\eta] \quad (5.28)$$

where $[\eta]$ is a column vector, $[\eta]^t$ a row vector and $[B]$ the potential energy matrix of order $3N$, analogous to the coefficients b_{ij} . Equation (5.15) can be written

$$\begin{bmatrix} \ddot{\eta} \\ \eta \end{bmatrix} + [B] [\eta] = 0 \quad (5.29)$$

Equation (5.18) can be written

$$([B] - \lambda [E]) [\eta^0] = 0 \quad (5.30)$$

The secular equation (5.20) becomes

$$[B] - \lambda [E] = 0 \quad (5.31)$$

In order to determine the amplitudes the equation used is

$$([B] - \lambda_k [E]) [\eta_k^0] = 0 \quad (5.32)$$

The resulting l_{ik} coefficients formally are the eigenvectors of the matrix $[B]$ and the λ_k values formally are the eigenvalues of the matrix $[B]$. The $[l_{ik}]$ column vector matrices are normalized so that

$$[l_k]^t [l_k] = 1 \quad (5.33)$$

Since $[B]$ is a symmetric matrix ($b_{ij} = b_{ji}$) the eigenvectors are orthogonal

$$[l_j]^t [l_k] = 0 \quad j \neq k \quad (5.34)$$

The column vectors $[l_{ik}]$ written side by side form the matrix $[L]$ of order $3N$. Similarly, the $[L]$ matrix is orthogonal such that

$$[L]^t = [L]^{-1} \quad (5.35)$$

The $[B]$ matrix can be diagonalized by a similarity transformation using the $[L]$ matrix

$$[L]^{-1} [B] [L] = [\Lambda_B] \quad (5.36)$$

Since $[L]$ is an orthogonal matrix equation (5.36) can be written

$$[L]^t [B] [L] = [\Lambda_B] \quad (5.37)$$

The molecular vibration problem has been solved in terms of mass-weighted Cartesian co-ordinates. A more useful co-ordinate system is needed due to the form of the potential energy equations (5.13) and (5.28) which include cross terms $\eta_i \eta_j$ ($i \neq j$). The kinetic energy expressions (5.7) and (5.27) are simply the sum of squared terms $\eta_i \eta_i$. The required set of co-ordinates is called the normal co-ordinates, $Q_1, Q_2, Q_3, \dots, Q_{3N}$ which describe the Lagrangian equation parameters T and V as

$$2T = [\dot{Q}]^t [\dot{Q}] \quad (5.38)$$

and

$$2V = [Q]^t [\Lambda_B] [Q] \quad (5.39)$$

The change from mass-weighted Cartesian co-ordinates to normal co-ordinates is achieved by a linear transformation of the form

$$[\eta] = [L] [Q] \quad (5.40)$$

or

$$[Q] = [L]^t [\eta] \quad (5.41)$$

The Lagrangian equations of motion take the form

$$[\ddot{Q}] + [\Lambda_B] [Q] = 0 \quad (5.42)$$

with solutions

$$Q_i = Q_i^0 \sin (t\lambda^{\frac{1}{2}} + \delta) \quad (5.43)$$

The secular equation becomes

$$|[\Lambda_B] - \lambda [E]| = 0 \quad (5.44)$$

The solution of these equations yields the $3N - 6$ fundamental frequencies of vibration.

The method as outlined involves solution of the secular equation in terms of mass-weighted Cartesian co-ordinates and normal co-ordinates. The six co-ordinates describing translation and rotation were then set equal to zero.

Instead of using space-fixed co-ordinates it is more common to introduce molecule-fixed co-ordinates. The original co-ordinate set is reduced by six and the new set is defined by the set

$$s_1, s_2, s_3, \dots, s_{3N-6} \quad (5.45)$$

Such co-ordinates are called internal co-ordinates because they describe the internal configuration of the molecule without regard for its position in space. Internal co-ordinates measure changes in bond lengths and bond angles which are chemically interpreted as bond stretching and angle bending vibrations.

In matrix notation the potential energy is written

$$2V = [S]^t [F] [S] \quad (5.46)$$

where $[S]$ is a row vector of $3N-6$ internal co-ordinate elements and $[F]$ is the potential energy matrix. $[F]$ is a square matrix of order $3N-6$ whose elements are the restoring force constants

$$f_{ij} = \left(\frac{\partial^2 V}{\partial s_i \partial s_j} \right)_0 \quad (5.47)$$

The format of the $[F]$ matrix varies markedly depending on the choice of potential energy force field.

The derivation of the kinetic energy in terms of internal co-ordinates is much more complicated. In mass-weighted Cartesian co-ordinates the kinetic energy is

$$2T = [\dot{\eta}]^t [\dot{\eta}] \quad (5.48)$$

The linear transformation relating mass-weighted Cartesian co-ordinates to internal co-ordinates is

$$[\eta] = [R] [S] \quad (5.49)$$

The matrix $[R]$ is required to perform the linear transformation. However $[R]$ is not readily found but from the geometrical model the

matrix $[D]$ is available for the inverse transformation

$$[S] = [D][\eta] \quad (5.50)$$

$[D]$ is a $(3N-6)$ by $3N$ rectangular matrix so that the operation $[D]^{-1} = [R]$ is not valid. The product $[D][D]^t$ is a $(3N-6)$ by $(3N-6)$ square matrix which can be inverted. This product is called the $[G]$ matrix. The expression for the kinetic energy reduces to a more useful form

$$2T = [\dot{S}]^t [G]^{-1} [\dot{S}] \quad (5.51)$$

The $(3N-6)$ dimensional secular equation to be solved becomes

$$| [F] - \lambda [G]^{-1} | = 0 \quad (5.52)$$

or in the more simple Wilson's FG matrix notation

$$| [G][F] - \lambda [E] | = 0 \quad (5.53)$$

From the solution of equation (5.53) the frequencies of the normal modes of vibration are obtained (eigenvalues) and the $[L]$ matrix in its unnormalized form also (eigenvectors). The next step is to find a normalization matrix $[N]$ for the unnormalized $[L]$ matrix according to

$$[L] = [A][N] \quad (5.54)$$

The $[N]$ matrix is a diagonal matrix whose elements are the numbers required to normalize the amplitudes of the $[A]$ matrix elements. It is found from the expression

$$[N]^2 = ([A]^t)^{-1} [G] [A]^{-1} \quad (5.55)$$

The $[N]$ matrix is then the square root of the above expression.

Potential Energy Functions

The purpose of a normal co-ordinate analysis is to determine the restoring force constants of a molecule along with the normal co-ordinates. Relatively few spectra have been subject to rigorous vibrational analyses. Simplicity of the molecular model is of great importance in the success of a detailed analysis. The calculation for many-atomed systems is hindered by the fact that the number of force constants in the potential energy function usually exceeds the number of observed fundamentals. Therefore, depending on the required accuracy of the force constant calculation, a suitable force field is chosen.

One of the more simple force fields available is the Central Force Field. The forces are assumed to act only along the lines joining each pair of atoms in their equilibrium positions. This would be a good potential field if the atoms were held together purely by ionic forces. The force constant matrix has only elements along the diagonal and no off-diagonal interaction terms. This force field is reasonably good for diatomic molecules but is rather bad for polyatomic systems.

A force field which gives a more descriptive potential environment is the Valence Force Field approximation. The restoring forces in this case are those which resist the extension or compression of valence bonds and those which resist the bending or torsion of bonds. Non-bonded interaction force constants are not considered. At best this force field is only a rough approximation. Deviations as high as 10% are quite usual. They do, however, give reasonable characteristic force constant values for bonds regardless of their environment. In this sense the force field is useful.

The force field chosen for this calculation is that of H. C. Urey and C. A. Bradley termed the Urey-Bradley Force Field (UBFF) (6). It is constructed basically from the valence force type function with additional terms to describe the existence of restoring forces between pairs of non-bonded atoms. Its simplicity enables the transfer of force constant values from one molecule to another to a good approximation in order to reduce the number of unknown

force constants to a workable size. No quadratic cross terms are employed but they are implicit in the interactions between non-bonded atoms. The UBFF has proven to be quite useful and accurate as demonstrated by such workers as Shimanouchi, Overend, Scherer, and others (24, 7).

The function has the form

$$V = \sum_i \{ \frac{1}{2} K_i (\Delta r_i)^2 + K_i' r_i (\Delta r_i) \} + \sum_{i < j} \{ \frac{1}{2} H_{ij} r_{ij}^2 (\Delta \alpha_{ij})^2 + H_{ij}' r_{ij}^2 (\Delta \alpha_{ij}) \} + \sum_{i < j} \{ \frac{1}{2} F_{ij} (\Delta q_{ij})^2 + F_{ij}' q_{ij} (\Delta q_{ij}) \} \quad (5.56)$$

where Δr_i , Δq_{ij} and $\Delta \alpha_{ij}$ are the changes in bond length, in the distance between non-bonded atoms and in the bond angle while K_i , K_i' , H_{ij} , H_{ij}' , F_{ij} , and F_{ij}' are the stretching, bending and repulsive force constants respectively. Also, the factors $r_{ij} = (r_i r_j)^{\frac{1}{2}}$, r_i and q_i make the force constants dimensionally the same.

Force Constant Calculation on a Digital Computer

The method employed in this treatment was developed by Overend and Scherer in 1960 (7). It is basically a perturbation type approach to the calculation of Urey-Bradley force constants from the observed vibrational frequencies.

In terms of internal co-ordinates the potential energy is

$$2V = [S]^t [F] [S] \quad (5.46)$$

where the $[F]$ matrix elements are linear combinations of the Urey-Bradley force constants

$$F_j^i = \sum_k a_{jk}^i \phi_k \quad (5.57)$$

The coefficients a_{jk}^i are available from the geometrical parameters. In (5.46) the $[F]$ matrix elements are arbitrarily arranged as a vector f , called the F-index vector, and the individual elements of $[F]$ are similarly arranged as a second vector F such that a one-to-one

mapping of index vectors f and F is achieved. For CSC1Br the arrangement is

$$[F] = \begin{bmatrix} f_1 & f_2 & f_4 & f_7 & f_{11} & f_{16} \\ . & f_3 & f_5 & f_8 & f_{12} & f_{17} \\ . & . & f_6 & f_9 & f_{13} & f_{18} \\ . & . & . & f_{10} & f_{14} & f_{19} \\ . & . & . & . & f_{15} & f_{20} \\ . & . & . & . & . & f_{21} \end{bmatrix} \quad (5.58)$$

A transformation matrix $[Z]$ is defined as

$$[F] = [Z][\phi] \quad (5.59)$$

where $[\phi]$ is a column vector of Urey-Bradley force constants. The ordering of the $[F]$ and $[Z]$ elements are determined by the f vector. The information contained in the F -index vector, f , is used to rearrange the F vector into the $[F]$ matrix.

The Urey-Bradley force field is a function of Δr_i , $\Delta \alpha_{ij}$ and Δq_{ij} which are not independent co-ordinates. By taking the first derivative of equation (5.56) equal to zero it is not justifiable to set the $(\partial V / \partial r_i)$, $(\partial V / \partial \alpha_{ij})$ and the $(\partial V / \partial q_{ij})$ terms also equal to zero. The redundant co-ordinates Δq_{ij} can be removed by an expression developed by Shimanouchi (24),

$$\begin{aligned} \Delta q_{ij} = & s_{ij}(\Delta r_i) + s_{ji}(\Delta r_j) + (t_{ij}t_{ji})^{1/2}(r_i/r_j)^{1/2}(r_i\Delta\alpha_{ij}) \\ & + \frac{1}{2}q_{ij} \{ t_{ij}^2(\Delta r_i)^2 + t_{ji}^2(\Delta r_j)^2 - s_{ij}s_{ji}(r_j/r_i)(r_i\Delta\alpha_{ij})^2 \\ & - 2t_{ij}t_{ji}(\Delta r_i\Delta r_j) + 2t_{ij}s_{ji}(r_j/r_i)(r_i r_i \Delta\alpha_{ij}) \\ & + 2t_{ji}s_{ij}(\Delta r_i r_i \Delta\alpha_{ij}) \} \end{aligned} \quad (5.60)$$

where

$$q_{ij}^2 = r_i^2 + r_j^2 - 2r_i r_j \cos \alpha_{ij} \quad (5.61)$$

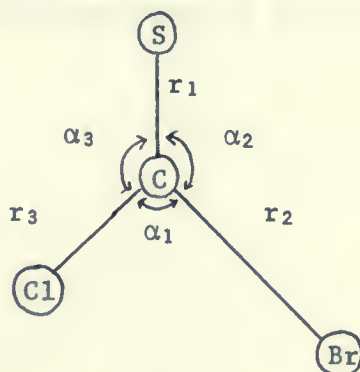
$$s_{ij} = (r_i - r_j \cos \alpha_{ij})/q_{ij} \quad s_{ji} = (r_j - r_i \cos \alpha_{ij})/q_{ij}$$

$$t_{ij} = (r_j \sin \alpha_{ij})/q_{ij} \quad t_{ji} = (r_i \sin \alpha_{ij})/q_{ij}$$

The potential function can then be expressed in terms of a set of independent co-ordinates such that $\partial V/\partial r_i$ and $\partial V/\partial \alpha_{ij}$ may be equated to zero. The final form of the potential energy function is

$$\begin{aligned} 2V = & \sum_i \{K_i + \sum_{i \neq j} t_{ij}^2 F'_{ij} + s_{ij}^2 F_{ij}\} (\Delta r_i)^2 \\ & + \sum_{i < j} \{H_{ij} - s_{ij} s_{ji} F'_{ij} + t_{ij} t_{ji} F_{ij}\} (r_{ij} \Delta \alpha_{ij})^2 \\ & + \sum_{i < j} \{-t_{ij} t_{ji} F'_{ij} + s_{ij} s_{ji} F_{ij}\} (\Delta r_i) (\Delta r_j) \\ & + \sum_{i < j} \{t_{ij} s_{ji} F'_{ij} + t_{ji} s_{ij} F_{ij}\} (r_j/r_i)^{1/2} (\Delta r_i) (r_{ij} \Delta \alpha_{ij}) \end{aligned} \quad (5.62)$$

In equation (5.62) the linear force constants F'_{ij} are introduced which makes it necessary to assume that $F'_{ij} = -0.1 F_{ij}$ as outlined by Shimanouchi et al. (25). This assumption reduces the number of force constants from twelve to nine for the CSClBr model. The molecular model for the force constant calculation is



The rows of the $[Z]$ matrix are obtained from the f vector and the columns obtained from the Urey-Bradley force constant matrix according to equation (5.59). Therefore, there are twenty-one row vectors and nine column vectors which form the $[Z]$ matrix.

		9 columns								
		K_{CS}	K_{CBr}	K_{CCl}	H_{ClBr}	H_{SBr}	H_{SCl}	F_{ClBr}	F_{SBr}	F_{SCl}
f_1	$(\Delta r_1 \Delta r_1)$
f_2	$(\Delta r_1 \Delta r_2)$
f_3	$(\Delta r_2 \Delta r_2)$
	.		.						.	
	.		.						.	
	.		.						.	
	.		.						.	
f_{21}	$(\Delta \alpha_3 \Delta \alpha_3)$

The $[F]$ matrix is reduced to its required $(3N-6)$ square matrix form by relating the f_n ($n=1,2,3,\dots,21$) elements to the f_{ij} ($ij=1,2,3,\dots,6$) elements. The relationships are of the type

$$\begin{aligned}
 n &= j(j-1)/2 + i & \text{if } i < j \\
 n &= i(i+1)/2 & \text{if } i = j \\
 n &= i(i-1)/2 + j & \text{if } i > j
 \end{aligned}
 \tag{5.63}$$

where i and j are the indices given by the internal co-ordinates in equation (5.47).

Urey-Bradley Force Constant Refinement

According to equation (5.59) $[F] = [Z][\Phi]$, an initial Urey-Bradley force constant matrix $[\Phi]$ is required to find $[F]$. The exact force constants composing the vector $[\Phi]$ are not known in advance, but rather are approximated by transferring appropriate U.B. force constants from similar molecules. That is, the refinement of the calculated force constants must begin with nine assumed force constants. The initial set of transferred force constants is given in Table 5.1. The roots of the secular equation (5.53) do not exactly equal the observed vibrational frequencies. A first order perturbation theory is used to refine the assumed force constants so that the agreement between observed and calculated frequencies is improved. A correction is sought for $[F]$ and hence $[\Phi]$ such that

$$\{\lambda_i^{(\text{calc.})} - \lambda_i^{(\text{obs.})}\} = 0 \quad (5.64)$$

Since the $[F]$ matrix elements are linear functions of the Urey-Bradley force constants through the relationship (5.59) and since the $[Z]$ matrix is simply an array of geometry dependent elements, the difference equation is valid in the form

$$[\Delta F] = [Z][\Delta \Phi] \quad (5.65)$$

The Jacobian matrix $[J^\Phi]$ is defined as the matrix whose elements are given by

$$J_{lk}^\Phi = \left(\frac{\partial \lambda_l}{\partial \phi_k} \right) \quad (5.66)$$

If the $(i-1)^{\text{th}}$ set of force constants is $[\phi]_{i-1}$ and the corresponding calculated roots are $[\lambda]_{i-1}$ the difference matrix $[\epsilon]_{i-1}$ is

$$[\epsilon]_{i-1} = [\lambda^{\text{obs}}]_{i-1} - [\lambda^{\text{calc}}]_{i-1} \quad (5.67)$$

A correction to the $(i-1)^{\text{th}}$ force constant set $[\Delta \phi]_{i-1}$ is required ac-

cording to

$$[J \phi] [\Delta \phi]_{i-1} = [\epsilon]_{i-1} \quad (5.68)$$

To obtain the final set of force constants several cycles of refinement are usually necessary until further refinement produces no change in the resulting force constants. For each cycle the $[\phi]$ matrix is adjusted by a small amount. In particular, for the $(i-1)^{th}$ cycle a set of residuals is obtained

$$[r]_{i-1} = [J \phi] [\Delta \phi]_{i-1} - [\epsilon]_{i-1} \quad (5.69)$$

The sum of the squares of this set of residuals is given by

$$X = [r]_{i-1}^t [W] [r]_{i-1} \quad (5.70)$$

where $[W]$ is the weight matrix of only diagonal elements defined by

$$W_{ii} = (1/\lambda_{ii}^{obs})^2 \quad (5.71)$$

The weight matrix fits the calculated roots to the observed roots on a percentage basis. When a frequency was not observed experimentally a weight matrix element was assigned as $W_{ii} = 0$. Substituting (5.69) into (5.70) and rearranging yields

$$X = [\Delta \phi]^t [J \phi]^t [W] [J \phi] [\Delta \phi] - [\epsilon]^t [W] [J \phi] [\Delta \phi] \quad (5.72)$$

The procedure is to then minimize X by differentiating with respect to

$$\partial X / \partial (\Delta \phi) = [\Delta \phi]^t [J \phi]^t [W] [J \phi] - [\epsilon]^t [W] [J \phi] = 0 \quad (5.73)$$

or

$$[\Delta \phi]_{i-1} = \{ [J \phi]^t [W] [J \phi] \}^{-1} [J \phi]^t [W] [\epsilon]_{i-1} \quad (5.74)$$

The i^{th} set of force constants then becomes

$$[\Phi]_i = [\Phi]_{i-1} + [\Delta\Phi]_{i-1} \quad (5.75)$$

The cycling procedure is then continued until $X = 0$. At this point for the k^{th} set of force constants

$$[\Delta\Phi]_k = 0$$

The matrix $[J^\phi]$ is called the Jacobian matrix. It can be obtained from the $[L]$ and the $[Z]$ matrices through the following relationship

$$[J^\phi] = [L]^t [Z] [L] \quad (5.76)$$

The Wilson's $[G]$ Matrix

The $[G]$ matrix is the kinetic energy matrix. Setting this matrix up for a computer calculation requires a rather lengthy algebraic operation during which errors are easily made. In non-matrix form the $[G]$ matrix elements are defined by

$$G_{tt'} = \sum_{i=1}^{3N} (1/m_i) B_{ti} B_{t'i} \quad (5.77)$$

where m_i is the mass of the i^{th} atom and the constants B_{ti} determined by the geometry of the molecule such that

$$S_t = \sum_{i=1}^{3N} B_{ti} \xi_i \quad (t=1, 2, 3, \dots, 3N-6) \quad (5.78)$$

For each atom α a vector $\vec{\rho}_\alpha$ whose components in three dimensional space are the three displacement co-ordinates ξ_i , $\xi_{i'}$, and $\xi_{i''}$, is introduced. For a given internal co-ordinate S_t the constants B_{ti} are grouped into threes; B_{ti} , $B_{ti'}$, and $B_{ti''}$. These quantities can be considered as the components of a vector $\vec{s}_{t\alpha}$ associated with the atom α and with the internal co-ordinate S_t . Equation (5.78) becomes

$$S_t = \sum_{\alpha=1}^N \vec{s}_{t\alpha} \cdot \vec{\rho}_\alpha \quad (5.79)$$

where the dot product is a scalar quantity. The direction of \vec{s}_t is chosen such that a maximum increase in S_t will be achieved and the magnitude $|\vec{s}_{t\alpha}|$ is equal to the increase in S_t upon unit displacement of atom α provided the other $N-1$ atoms are fixed in their equilibrium positions. Instead of the $3N$ coefficients B_{ti} (for each S_t) it is more convenient to use the N vectors $\vec{s}_{t\alpha}$. Therefore, equation (5.77) is written

$$G_{tt'} = \sum_{\alpha=1}^N \mu_\alpha \vec{s}_{t\alpha} \cdot \vec{s}_{t'\alpha} \quad (5.80)$$

where μ_α is the reduced mass of the α atom. One element $G_{tt'}$ occurs for each pair of internal co-ordinates S_t and $S_{t'}$, and no co-ordinate axes are necessary if the \vec{s} vectors are easily described. The \vec{s} vectors can be described in terms of bond vectors and other simple unit vectors so that the scalar products of the \vec{s} vectors can be reduced to a sum of scalar products of certain unit vectors (bond vectors) within the molecule. These vectors may be substituted into Wilson's formulas for bond stretching and angle bending internal co-ordinates (26).

Urey - Bradley Force Constants for CSClBr

The calculation of vibrational frequencies and normal co-ordinates from the force constants is a straight forward procedure. In practice, however, it is the vibrational frequencies that are observed, and the force constants and normal co-ordinates that we wish to determine. This reverse calculation is much more difficult. Almost all force constant calculations these days are performed using the force constant refinement procedure. The force constants are obtained by an iterative method, in which some set of approximate constants are made to converge upon the true force constants via the Jacobian matrix $[J^{\phi}]$

A normal co-ordinate calculation is basically dependent upon the molecular geometry. The molecular model used in this calculation is only an approximate description of the exact geometry since no microwave or electron diffraction data is available at present. The approximate parameters were

$$\begin{array}{ll} r(C=S) = 1.63 \overset{O}{A} & (ClCBr) = 110.7^{\circ} \\ r(C-Cl) = 1.746 \overset{O}{A} & (SC Br) = 125^{\circ} \\ r(C-Br) = 2.05 A & (SCCl) = 124.3^{\circ} \end{array}$$

where the bond lengths and angles are those transferred from $CSCl_2$, $COClBr$ and $COBr_2$ (15,7). The atomic weights of the weights of the carbon, sulphur, chlorine and bromine atoms were taken to be 12.0, 31.97207, 34.96885 and 78.9183 respectively. The initial set of Urey-Bradley force constants were those transferred from $CSCl_2$ and $COClBr$ as given in Table 5.1.

TABLE 5.1

Initial Set of Transferred Urey-Bradley Force Constants		
Force Constant Symbol	Value (m dyn/Å)	Source
$K_{C=S}$	5.44	(a)
K_{CBr}	1.565	(b)
K_{CCl}	2.30	(a)
H_{ClBr}	0.07	(b)
H_{SBr}	0.101	(d)
H_{SCl}	0.101	(c)
F_{ClBr}	0.525	(b)
F_{SBr}	0.681	(d)
F_{SCl}	0.681	(c)

(a) Reference 15

(b) Reference 7

(c) Reference 12

(d) Assumed to be at least the same as the analogous chlorine force constant.

Table 5.2 lists the calculated Wilson's $[G]$ matrix elements for $CS^{35}Cl^{79}Br$. Table 5.3 lists the calculated $[Z]$ matrix elements for $CSClBr$. This matrix is a 21 X 9 array corresponding to the nine Urey-Bradley force constants. The force constant refinement difficulty arises from

the fact that there are nine in-plane force constants but only five in-plane frequencies of vibration for the molecule. The experimental data was therefore not sufficient to uniquely determine the Urey-Bradley force constants. This is usually the case for force constant calculations of polyatomic molecules. We attempted to choose the most probable set of force constants from a rather large number of possible solutions. We did this by reducing the number of force constants which we could vary in the calculation from nine to five, in order to match the number of observed frequencies. Two force constants were transferred from CSCl_2 . They were H_{SCl} and F_{SCl} with values of 0.101 and 0.681 m-dyne/Å respectively. One force constant was transferred from COCIBr , its symbol and value being H_{ClBr} and 0.07 m-dyne/Å respectively. These three force constants were constrained: that is, forced to take these values in all the refinement calculations. The final set of force constants chosen should be the most reliable since it correlates very well with the force constants obtained for CSF_2 and CSCl_2 . Both these molecules are of C_{2v} symmetry and their force constant calculations were greatly aided by the fact that there were only six different force constants to match with the five observed frequencies.

Thus by varying five of the six non-constrained force constants in each refinement to achieve convergence of the observed versus calculated frequencies (to $\pm 5 \text{ cm}^{-1}$) we obtained our best choice for the set of Urey-Bradley force constants given in Table 5.4. This set of force constants gave the calculated frequencies listed in Table 5.5.

The calculated frequencies are the eigenvalues of the secular equation (5.53) and the corresponding eigenvectors normalized to give the $[L]$ matrix are listed in Table 5.6.

TABLE 5.2

[G] Matrix Elements for CS ³⁵ Cl ⁷⁹ Br					
0.11458330	-0.04779832	-0.04696082	0.07272690	-0.039428190	-0.03329876
-0.04779832	0.09599149	-0.029455820	-0.04464678	0.08652555	-0.04187881
-0.04696082	-0.029455820	0.111904700	-0.03802599	-0.042234130	0.08026009
0.07272690	-0.044646780	-0.038025990	0.076008370	-0.04713368	-0.02887468
-0.039428190	0.086525550	-0.0422341300	-0.0471336800	0.11283590	-0.06570231
-0.033298760	-0.0418788100	0.080260090	-0.028874680	-0.06570231	0.094577010

TABLE 5.3

The $[Z]$ Matrix Elements for CSClBr

f-index vector	K_{CS}	K_{CBr}	K_{CCl}	H_{ClCBr}	H_{BrCS}	H_{ClCS}	F_{ClBr}	F_{BrS}	F_{ClS}
1	1.00							0.743246	0.709904
2									0.804242
3		1.00					0.700002		0.816596
4									
5							0.705701		
6			1.00				0.586441		
7									
8							0.840955		
9							0.738511		
10				3.579300			1.387246		
11								0.614211	
12									
13								0.6398484	
14									
15					2.845980			0.842556	
16									0.622162
17									0.706998
18									
19									
20									
21						3.341500			0.962419

TABLE 5.4
Urey-Bradley Force Constants for CSClBr

Force Constant	Value
Symbol	m.dyne/Å
$K_{C=S}$	5.319
K_{CBr}	1.96
K_{CCl}	2.331
* H_{ClBr}	0.07
H_{SBr}	0.066
* H_{SCl}	0.101
F_{ClBr}	0.726
F_{SBr}	0.55
* F_{SCl}	0.681

TABLE 5.5
 Observed and Calculated in-plane Frequencies
 for CS³⁵Cl⁷⁹Br

Frequency	Observed (cm ⁻¹)	Calculated (cm ⁻¹)	Difference (cm ⁻¹)
ν_1	1130	1129.2	0.8
ν_2	764	763.1	0.9
ν_3	438	440.4	2.4
ν_4	256	256.0	0.0
ν_5	222	224.8	2.8

* Force constant constrained

TABLE 5.6

The $[L]$ Matrix Elements of ^{35}CS ^{79}Cl Br

	Matrix Elements for Modes				
	ν_1	ν_2	ν_3	ν_4	ν_5
∂r_{CS}	.3351134	.0323107	-.0337040	-.0034372	-.0030833
∂r_{CBr}	-.1349528	-.2367020	-.1400156	.0236462	-.0451941
∂r_{CCl}	-.1744707	.2718214	-.0840632	.0127074	.0142770
$\partial \theta_{\text{ClCBr}}$.2254136	.0234559	.0836509	.1339137	.0155194
$\partial \theta_{\text{BrCS}}$	-.1050044	-.2361805	-.1228858	-.0681943	.1138661
$\partial \theta_{\text{ClCS}}$	-.1201272	.2398087	.0394824	-.0656936	-.1291739

Chapter 6

Approximate Self-Consistent Molecular Orbital Theory (The CNDO Method) (27,28,29)

The electronic energy states E_E of a polyatomic molecule are eigenstates of the Hamiltonian operator H_E satisfying the quantum mechanical relationship

$$H_E \Psi_E = E_E \Psi_E \quad (6.1)$$

The total electronic wave function Ψ_E is set up in terms of a set of basis functions. Most applications use linear combinations of atomic orbitals (L.C.A.O.) Each molecular orbital (MO) can be constructed as a linear combination of atomic orbitals

$$\Psi_i = \sum_{\nu} c_{\nu i} \phi_{\nu} \quad (6.2)$$

where ϕ_{ν} are valence atomic orbitals and $c_{\nu i}$ the orbital coefficients. If the coefficients in the LCAO orbitals are chosen to minimize the total energy one obtains LCAO/MO/SCF orbitals, the best LCAO approximations to the self consistent functions.

Without further approximation this technique is limited by computational difficulties in the treatment of large molecules. The "neglect of differential overlap" approximation has been developed for the π electrons only of aromatic systems. The Pople, Santry and Segal method employs self consistent techniques based on neglect of differential overlap for all valence orbitals.

According to Roothaan's LCAO/SCF treatment only electrons in the valence shell are considered explicitly, all inner shells being treated as part of an unpolarizable core. For closed shell configurations, variational treatment of the orbital coefficients yields the basic equations

$$\sum_{\nu} F_{\mu\nu} c_{\nu i} = \sum_{\nu} S_{\mu\nu} c_{\nu i} \epsilon_i \quad (6.3)$$

where

$$F_{\mu\nu} = H_{\mu\nu} + G_{\mu\nu} \quad (6.4)$$

and

$$S_{\mu\nu} = \int \bar{\phi}_\mu \phi_\nu d\tau \quad (6.5)$$

In these equations ϵ_i is the orbital energy for the molecular orbital ψ_i and $H_{\mu\nu}$ is the matrix element of the one-electron Hamiltonian including the kinetic energy and the potential energy in the electrostatic field of the core. $G_{\mu\nu}$ is the matrix element of the potential due to other valence electrons and depends upon the molecular orbitals via the population matrix $P_{\lambda\sigma}$ over the occupied molecular orbitals only,

$$P_{\lambda\sigma} = 2 \sum_i^{\text{occ}} \bar{c}_{i\lambda} c_{i\sigma} \quad (6.6)$$

The orbital energies ϵ_i are roots of the secular equation

$$| F_{\mu\nu} - \epsilon S_{\mu\nu} | = 0 \quad (6.7)$$

and the total electronic energy of the valence electrons is

$$E_{\text{electronic}} = \frac{1}{2} \sum_{\mu\nu} P_{\mu\nu} (H_{\mu\nu} + F_{\mu\nu}) \quad (6.8)$$

The total energy of the molecule (relative to separated valence electrons and isolated cores) is obtained by adding the repulsion energy between cores. This energy can be approximated by a point charge model so that

$$E_{\text{total}} = E_{\text{electronic}} + \sum_{A < B} \sum_{B} \frac{Z_A Z_B}{R_{AB}} \quad (6.9)$$

where Z_A is the core charge on atom A and R_{AB} the internuclear distance. Equation (6.3) can be written in matrix notation

$$[F][c_i] = ([H] + [G])[c_i] = [S][c_i]\epsilon_i \quad (6.10)$$

where $[F]$ and $[S]$ are the matrices of $F_{\mu\nu}$ and $S_{\mu\nu}$ respectively and $[c_i]$ is the column matrix $c_{\nu i}$ and ϵ_i the orbital energy, a scalar quantity.

Molecular wavefunctions formed from the antisymmetrized products of one-electron wavefunctions are invariant with respect to an orthogonal transformation of the occupied molecular orbitals among themselves. These molecular wavefunctions and the corresponding ϵ_i are also invariant with respect to an orthogonal (or unitary) transformation between the atomic

orbital basis functions. A new basis set of functions t_m is chosen related to the original set ϕ_μ by the matrix equation

$$[t] = [O][\phi] \quad (6.11)$$

where $[O]$ is an orthogonal transformation matrix. Equation (6.10) becomes

$$\{[O]^{-1}[H'][O] + [O]^{-1}[G'][O]\}[c_i] = [O]^{-1}[S'][O][c_i]\epsilon_i \quad (6.12)$$

where H' , G' and S' are referred to the new basis set t . The elements of the electron repulsion matrix G' and the Hamiltonian are given by

$$G'_{mn} = \sum O_{m\mu} O_{n\nu} G_{\mu\nu} \quad (6.13)$$

and

$$H'_{mn} = \sum O_{m\mu} O_{n\nu} H_{\mu\nu} \quad (6.14)$$

Possible transformations may be classified in increasing degree of complexity by

- (i) Transformations which only mix 2px, 2py and 2pz atomic orbitals centered on the atom;
- (ii) Transformations which only mix 2s and 2p orbitals on the same atom;
- (iii) General transformations which mix atomic orbitals on different atoms (leading to a nonatomic basis set)

The first type corresponds to a rotation of local atomic axes, an essential invariance feature for molecules of low symmetry. The second transformation corresponds to the hybridization of the orbitals on the various atoms. Although the choice of a particular hybrid form does not strictly make any difference to the calculation of the electronic structure of a molecule, the concept is very useful.

The approximate molecular orbital theory with complete neglect of differential overlap between orbitals on the same atom has five basic approximations.

- (1) If the ϕ 's form an orthonormal set the overlap integrals

$S_{\mu\nu}$ are zero unless $\mu=\nu$ in which case they equal unity. The coefficients $c_{i\mu}$ then form an orthogonal matrix and the orthonormality

condition for Ψ_i becomes

$$\sum_{\mu} c_{i\mu} c_{\mu j} = \delta_{ij} \quad (6.15)$$

where

$$\begin{aligned} \delta_{ij} &= 1 & \text{for } i = j \\ \delta_{ij} &= 0 & \text{for } i \neq j \end{aligned}$$

(2) All two-electron integrals of the type

$$G_{\mu\nu} = \sum_{\lambda\sigma} P_{\lambda\sigma} \{ (\mu\nu|\lambda\sigma) - \frac{1}{2} (\mu\sigma|\nu\lambda) \} \quad (6.16)$$

which depend on the overlapping of charge densities of different basis orbitals are neglected. This means that the integral $(\mu\nu|\lambda\sigma)$ is zero unless $\mu=\nu$ and $\lambda=\sigma$. As a result of this approximation the theory becomes invariant which necessitates further approximations.

(3) The electron interaction integrals are assumed to depend only on the atoms to which the M.O.'s ϕ_{μ} and ϕ_{ν} belong and not to the actual type of orbital. Hence, there remains only a set of atomic electronic-interaction integrals measuring an average repulsion between an electron in a valence atomic orbital on atom A and another valence atomic orbital on Atom B. In this manner the diagonal core matrix elements are written.

$$H_{\mu\mu} = U_{\mu\mu} - \sum_{B \neq A} (\mu|V_B|\mu) \quad (6.17)$$

where $U_{\mu\mu}$ is the diagonal matrix element of ϕ_{μ} with respect to the one-electron Hamiltonian containing only the core of its own atom. The off-diagonal core matrix elements $H_{\mu\nu}$ may be written if ϕ_{μ} and ϕ_{ν} are on the same atom (A) in a similar manner,

$$H_{\mu\nu} = U_{\mu\nu} - \sum_{B \neq A} (\mu|V_B|\nu) \quad (6.18)$$

where again $U_{\mu\nu}$ is the one-electron matrix element using the local core Hamiltonian. By symmetry it is zero if ϕ_μ and ϕ_ν are s,p,d functions. The remaining terms of equation (6.18) represent the interaction of the distribution $\phi_\mu\phi_\nu$ with cores of other atoms. Since corresponding electron interaction integrals are neglected, it is consistent to neglect these contributions.

(4) Integrals $(\mu|v_B|\nu)$ where ϕ_μ and ϕ_ν belong to atom A are zero if $\mu \neq \nu$. Also, if ϕ_μ and ϕ_ν are the same the integral is the same for all valence atomic orbitals on A so that

$$(\mu|v_B|\nu) = v_{AB} \quad (6.19)$$

where the matrix v_{AB} need not be symmetric. For s, p, d, basis functions

$$H_{\mu\mu} = U_{\mu\mu} - \sum_{B(\neq A)} v_{AB} \quad (\mu \text{ on atom A}) \quad (6.20)$$

and

$$H_{\mu\nu} = 0 \quad (\mu \neq \nu, \text{ but both on the same atom}) \quad (6.21)$$

For ϕ_μ and ϕ_ν on different atoms the assumption is again the distribution $\phi_\mu\phi_\nu$ with distant cores is neglected and that the Hamiltonian $H_{\mu\nu}$ is a measure of the possible lowering of energy levels by being in the electrostatic field of two atoms simultaneously. $H_{\mu\nu}$ is then denoted as the "resonance integral" $\beta_{\mu\nu}$ estimated by approximation (5).

(5) Off-diagonal core matrix elements between atomic orbitals on different atoms are estimated by the formula

$$H_{\mu\nu} = \beta_{\mu\nu} = \beta_{AB}^0 S_{\mu\nu} \quad (6.22)$$

where $S_{\mu\nu}$ is the overlap integral and β_{AB}^0 is a parameter depending only on the nature of atoms A and B.

To elaborate on the actual calculation, the basis set consists of Slater type orbitals for the valence shell where for example any 1s orbital is given by

$$1s = (Z'^3/\pi)^{1/2} \exp(-Z'r) \quad (6.23)$$

where the Slater values Z' are constants for the valence shell of the atoms concerned. The electron repulsion integral γ_{AB} , representing the interaction between electrons in valence atomic orbitals on atoms A and B, is calculated as the two-center Coulomb integral involving valence s functions or

$$\gamma_{AB} = \iint s_A^2(1)(r_{12})^{-1} s_B^2(2) d\tau_1 d\tau_2 \quad (6.24)$$

for which formulas are listed. The parameters β_{AB}^0 are obtained from the formula

$$\beta_{AB}^0 = \frac{1}{2} (\beta_A^0 + \beta_B^0) \quad (6.25)$$

where β_A^0 are determined empirically so that the CNDO calculations give the best LCAO-SCF calculations for diatomics.

The CNDO/2 Approximations:

(1) The original CNDO theory predicted diatomic bond lengths consistently too small and binding energies consistently too large. This was due to a "penetration effect" in which the electrons in an orbital on one atom penetrate the shell of another atom leading to net attraction. The Hartree-Fock matrix $H_{\mu\mu}$ can be rewritten ignoring the terms described by the penetration effect. This approximation is not completely justified but it does improve the calculation while simplifying it at the same time.

(2) The CNDO estimation of $U_{\mu\mu}$ the local core matrix element was achieved through the atomic ionization potential I_μ by the relation

$$-I_{\mu} = U_{\mu\mu} + (Z_A - 1)\gamma_{AA} \quad (6.26)$$

An alternative approach is to use atomic electron affinities

$$-A_{\mu} = U_{\mu\mu} + Z_A \gamma_{AA} \quad (6.27)$$

The CNDO/2 approximation is to average both the effects of equations (6.26) and (6.27) to account for the tendency of an atomic orbital to both acquire and lose electrons.

$$-\frac{1}{2}(I_{\mu} + A_{\mu}) = U_{\mu\mu} + (Z_A - \frac{1}{2})\gamma_{AA} \quad (6.28)$$

CNDO/2 Calculations:

The calculations using the CNDO/2 method were carried out with a computer program incorporating the theory outlined originally by Pople, Santry and Segal. The program consisted of an approximate 1000 card deck provided by the QCPE (Quantum Chemistry Program Exchange) located at Indiana University (30). The calculations were executed for the closed shell configurations on an IBM 360 computer. The input data consisted of the wavefunction option, the open-closed shell option, the number of atoms, the molecular charge, the multiplicity, the atomic number of the atoms and the Cartesian co-ordinates of the atoms in their experimental molecular geometry.

Equilibrium Geometries and Quadratic Force Constants:

The calculated CNDO/2 and experimental equilibrium geometries are listed in Table 6.I. for the series of molecules COH_2 , COF_2 , COCl_2 , CSH_2 , CSF_2 and CSCl_2 . The experimental geometries for the three carbonyl molecules COX_2 ($\text{X}=\text{H}, \text{F}, \text{Cl}$) are readily available and presumably accurate.

The quoted experimental bond lengths and angles of the thiocarbonyls, CSX_2 , ($\text{X} = \text{H}, \text{F}$ and Cl) are not as reliable and in many cases are assumed to be the same as the analogous carbonyl compounds.

The CNDO/2 theory was originally applied to AB_2 and AB_3 type molecules and has been shown to successfully predict equilibrium bond angles (29). It was then applied to diatomics and several polyatomics, including formaldehyde, which led to some success in the calculation of equilibrium bond lengths (31). In the present work we applied the method to the previously mentioned series since geometries of the carbonyl and thiocarbonyl halides are actually the very basis for ground state infrared and normal co-ordinate analysis calculations.

As outlined in the following section on CNDO/2 calculations of infrared band intensities, the molecular model is set up in terms of symmetrized internal co-ordinates. Our series of molecules has C_{2v} symmetry so that the stretching vibrations are of A_1 symmetry and the symmetrical bending vibrations are of B_2 symmetry. All equilibrium bond lengths were calculated by the uniform grid type variation of the length of bonds ranging from the smallest grid of $\pm 0.005 \text{ \AA}$ to the largest of $\pm 0.02 \text{ \AA}$. In a similar manner the bond angles were expanded and contracted at intervals of 2° . Under these vibration type conditions all other atoms were held fixed in their equilibrium positions. The symmetrized internal valence co-ordinates were defined by the equation

$$S_i = \frac{1}{n^{1/2}} \left(\sum_i \Delta q_i \right) \quad (6.29)$$

where Δq_i is the change in the i^{th} bond distance or angle. For the series of molecules XYZ_2 ($\text{Y} = \text{C}, \text{X} = \text{O}$ and $\text{S}, \text{Z} = \text{H}, \text{F}$ and Cl) where n is the number of equivalent YX or YZ bonds in the molecule the following defined vibrations were performed

$$\begin{array}{ll} \text{YX stretch} & S_1 = \frac{1}{1^{1/2}} \Delta r_{\text{YX}} = \Delta r_{\text{YX}} \\ \text{YZ stretch} & S_2 = \frac{1}{2^{1/2}} (\Delta r_{\text{YZ}} + \Delta r_{\text{YZ}}) = \frac{2}{2^{1/2}} (\Delta r_{\text{YZ}}) \\ \text{ZYZ bend} & S_3 = \frac{1}{2^{1/2}} (\Delta \alpha_{\text{ZYZ}}) = \frac{1}{2^{1/2}} (\Delta \alpha_{\text{ZYZ}}) \end{array} \quad (6.30)$$

The definition of the symmetrized internal co-ordinates is important

in calculating the appropriate force constants.

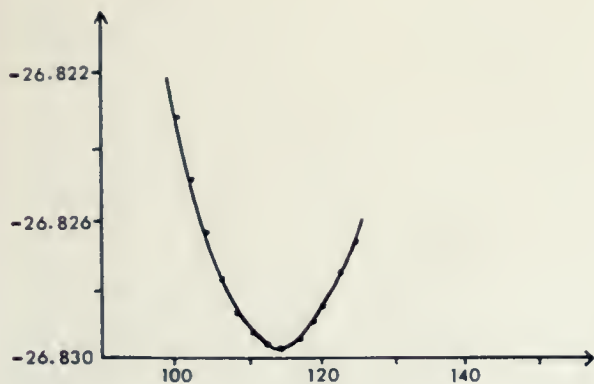
The CNDO/2 calculated geometries are obtained by plotting either the total energy or the electronic energy on the ordinate axis and the bond length or angle along the abscissa axis to obtain the potential energy curves. A few examples of these plots are shown in Figure 6.1. The calculated minima are generally not much different from the experimental equilibrium results so that the CNDO/2 calculations give a good representation of the geometry for the thiocarbonyl halides. Although the fact that the shapes of the potential curves are quite inaccurate the minima predictions are quite good.

The method as shown in Table 6.1 seems to reproduce the geometrical trends. Ignoring CSCl_2 , the obvious trend is that the bond lengths are longer than the experimental values and the symmetric bond angles are calculated to be smaller than experimental values. The one oddity in this trend is $r(\text{C-Cl})$ in COCl_2 which turns out to be shorter than the experimental result. This could be the true case but the experimental result seems also to be somewhat in doubt.

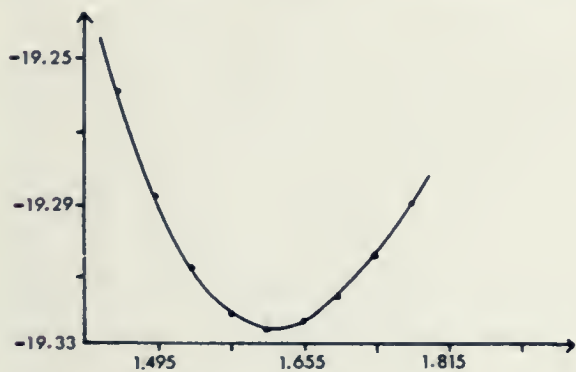
For the COX_2 ($\text{X}=\text{H}, \text{F}, \text{Cl}$) series the trend in C=O bond length is also reproduced, that is, the bond length decreases systematically for $\text{X}=\text{H}$ to $\text{X}=\text{F}$ to $\text{X}=\text{Cl}$. The C=O bond length for COH_2 is calculated to be 1.253\AA , for COF_2 1.250\AA and for COCl_2 , 1.246\AA . The differences with the experimental results are 0.05, 0.079 and 0.080 Å respectively. However, the experimental trend in the C=S bond lengths for the CSX_2 ($\text{X}=\text{H}, \text{F}, \text{Cl}$) series is not reproduced by the calculation. In particular the C=S bond length in CSF_2 is calculated to be longer than the C=S bond length in CSH_2 and CSCl_2 . From the experimental geometry and force constant data this bond in CSF_2 should be shorter. The differences between calculated and observed carbon chlorine bond lengths are 0.071\AA and 0.115\AA for phosgene and thiophosgene respectively which in the latter case is rather large. It is interesting to note that the carbon hydrogen bond length in formaldehyde and thioformaldehyde are calculated to be almost the same, 1.118 versus 1.120\AA respectively. The experimental geometries $r(\text{CH})$ and $\theta(\text{HCH})$ are also very similar.

The equilibrium bond angle calculations are in quite good agreement in the three molecules studied where experimental comparisons were possible. The largest difference is 2.1° in the case of the HCH angle of formaldehyde. Although seemingly trivial it is noteworthy that the CNDO/2 calculates

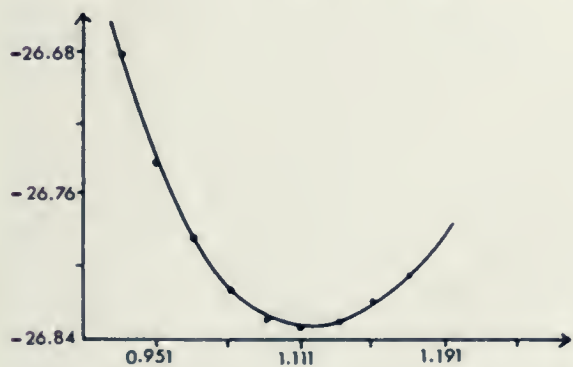
Figure 6.1: CNDO/2 calculated theoretical plots of total energy in atomic units along the ordinate axis versus bond lengths in Angstroms or bond angle in degrees along the abscissa axis for some C_{2v} molecules.



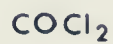
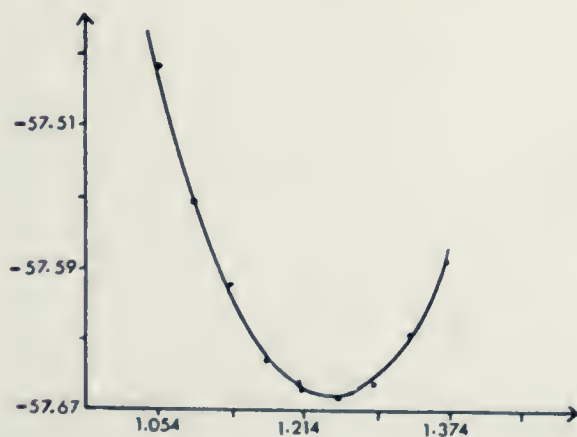
T.E.(AU) vs. HCH angle (°)



T.E.(AU) vs. C=S Bond Length (Å)



T.E.(AU) vs. C-H Bond Length (Å)



T.E.(AU) vs. C=O Bond Length (Å)

TABLE 6.I.

CNDO/2 Equilibrium Geometries

Molecule	Symmetrized Type of Vibration	Parameter	Parameter Value		
			CNDO/2	Experimental	
COH ₂	S ₁	r(C = O)	1.253Å	1.203Å	(a)
	S ₂	r(C - H)	1.118Å	1.101Å	
	S ₃	θ(H C H)	114.4°	116.5°	
COF ₂	S ₁	r(C = O)	1.250Å	1.171Å	(b)
	S ₂	r(C - F)	1.331Å	1.312Å	
	S ₃	θ(F C F)	107.0°	108.0°	
COCl ₂	S ₁	r(C = O)	1.246Å	1.166Å	(c)
	S ₂	r(C - Cl)	1.675Å	1.746Å	
	S ₃	θ(ClCCl)	(h)	111.3°	
CSH ₂	S ₁	r (C = S)	1.625Å	1.611Å	(d)
	S ₂	r (C - H)	1.120Å	1.089Å	
	S ₃	θ (H C H)	116.0°	116.7°	
CSF ₂	S ₁	r(C = S)	1.658Å	1.563±0.1Å	(d)
	S ₂	r(C - F)	1.326Å	1.285±0.01Å	(e)
	S ₃	θ(F C F)	111.5°	108 ±0.5°	(e)
CSCl ₂	S ₁	r(C = S)	1.600Å	1.630Å	(f)
	S ₂	r(C-Cl)	1.631Å	1.746Å	(g)
	S ₃	θ(ClCCl)	(h)	111.3°	(g)

(a) Reference 32

(b) Reference 33

(c) Reference 34

(d) Reference 35

(e) Reference 3

(f) Reference 15

(g) Assumed values from COCl₂

(h) Angle calculated to be less than 90°

Table - 6.2

QUADRATIC FORCE CONSTANTS

Molecule	Valence Force Field		Force Constant Value (mdyn-A^{-1})	
	Force	Constant	CNDO/2	Experimental
COH_2	K(C=O)	stretch	33.4	13.0
	K(CH)	stretch	12.0	5.2
	H(HCH)	bend	0.75	0.66
COF_2	K(C=O)	stretch	35.8	15.21
	K(CF)	stretch	17.1	6.48
	H(FCF)	bend	(a)	1.57
	H(FCO)	bend	(a)	1.09
COCl_2	K(C=O)	stretch	35.3	13.74
	K(CCl)	stretch	8.5	3.06
	H(ClCCl)	bend	(b)	0.96
	H(ClCO)	bend	(b)	0.79
CSH_2	K(C=S)	stretch	10.2	-
	K(CH)	stretch	8.9	-
CSF_2	K(C=S)	stretch	16.3	7.82
	K(CF)	stretch	16.0	5.93
	H(FCF)	bend	(a)	1.49
	H(FCS)	bend	(a)	0.92
CSCl_2	K(C=S)	stretch	13.4	6.34
	K(CCl)	stretch	9.0	3.36
	H(ClCCl)	bend	(b)	1.12
	H(ClCS)	bend	(b)	0.86

(a) Calculation not performed

(b) Potential function highly irregular

all the symmetrical angles to be properly less than the planar trigonal value of 120° .

The method of calculating the equilibrium bond lengths and angles also gave the quadratic force constant as a result. This method employs the fitting of a parabolic type equation to the potential curve. Three successive points were fitted to a parabola so that the midpoint had lower energy either end point. Thus the minimum yielded the equilibrium value from which the valence force constant could be calculated. Very small bond length and angle differences were used close to the minimum so that the harmonic component of the potential was estimated and other anharmonic components neglected. The parabola type equation took the form

$$V - \bar{V}_e = \frac{1}{2} K (x - \bar{x}_e)^2 \quad (6.31)$$

where \bar{V}_e and \bar{x}_e correspond to the minimum value of the energy and the equilibrium bond length or angle respectively. In this manner three sets of values for the total energy and bond parameter yielded the equilibrium bond length or angle and the valence force field force constant.

The results of the CNDO/2 force constant calculation are given in Table 6.2. They are consistently too large but it is interesting to note that the stretching constants are very nearly a factor of three times the experimental values. This is consistent with the results obtained by Segal (31). The calculation does however reproduce the important trends; namely, $K_{C=O}$ for COH_2 , COF_2 and COCl_2 remains relatively constant as do the experimental results. $K_{C=S}$ for CSF_2 is 16% larger than $K_{C=S}$ for CSCl_2 . The experimental difference is about 18%.

The values given in Table 6.2 for the experimental valence force field force constants are those obtained from our Fortran force constant program. The program calculates

$$[F] = [Z] [\Phi]$$

where $[\Phi]$ is the Urey-Bradley force constant matrix.

Calculation of Infrared Intensities by the CNDO/2 Method

Fundamental infrared band intensities can be measured experimentally by the method of Wilson and Wells, and Penner & Weber (36,37). The experimental integrated intensity for a particular fundamental is given by

$$\Gamma = \frac{1}{n l} \int_{\text{band}} \ln \frac{I_0}{I} d(\ln \nu) \quad (6.32)$$

where n is the sample concentration in moles per cubic centimeter, l is the absorbing path length in centimeters and I_0 and I the intensities of the incident and transmitted light of frequency ν . Γ has the units of square centimeters per mole. By the technique developed at the University of Minnesota gas phase intensity data has been transformed, to a very good approximation, into derivatives of the total molecular dipole moment with respect to defined symmetry coordinates (17). Intensity data have frequently been further interpreted in terms of bond moments and effective charges, although there are distinct limits to the validity of such interpretations.

As outlined in Chapter 2, the explicit relationship between the integrated intensity of a fundamental absorption band and the derivative of the molecular dipole moment with respect to a normal co-ordinate is given by

$$\Gamma_i = \frac{N \pi}{3 c^2 h} \left(\frac{\partial P}{\partial Q_i} \right)^2 \quad (6.33)$$

where

$$\left(\frac{\partial P}{\partial Q_i} \right)^2 = \left(\frac{\partial P_x}{\partial Q_i} \right)^2 + \left(\frac{\partial P_y}{\partial Q_i} \right)^2 + \left(\frac{\partial P_z}{\partial Q_i} \right)^2 \quad (6.34)$$

It is the derivative of the dipole moment with respect to the normal

co-ordinate which is sought in quantitative intensity studies.

The CNDO method, an approximate self-consistent molecular orbital theory, can be applied to the calculation of dipole moment derivatives $M_j = (\partial P / \partial S_j)$. If anharmonicity is ignored equation (6.33) predicts that the integrated intensity of a fundamental vibration-rotation band is temperature independent and is proportional to $(\partial P / \partial Q_i)^2$. The full SCF - LCAO - MO theory has been applied by Segal and Klein to molecules composed only of first row elements and hydrogen to give a reasonable approximation to the trends between these molecules and the magnitude of the dipole moments (38). Their attempt met with reasonable success so that an attempt was made by our group to apply the technique to a series of four-atom carbonyl and thiocarbonyl molecules of planar C_{2v} symmetry.

For convenience it is possible to obtain the change in dipole moment with respect to internal symmetry co-ordinates S_j , the appropriate transformation to normal co-ordinates being

$$M_j = \left(\frac{\partial P}{\partial S_j} \right) = \sum_i \left(\frac{\partial P}{\partial Q_i} \right) \left(\frac{\partial Q_i}{\partial S_j} \right) \quad (6.35)$$

where the derivatives can be obtained from the $[L]$ matrix through a normal co-ordinate analysis. Experimental determination of $(\partial P / \partial Q_i)$ leads to a sign ambiguity; that is, from the integrated intensity one obtains either a positive or a negative $(\partial P / \partial Q_i)$. This ambiguity gives rise to sets of solutions for the $(\partial P / \partial S_j)$ values obtained. Chemical intuition has been used to decrease the number of possible choices. However, the CNDO/2 method of determining yields only a single result (sign and magnitude) which possibly can be correlated with experimental results to resolve the sign ambiguity problem.

The CNDO/2 method describes the molecular dipole moment as the sum of two types of terms. One arises from a contribution of the net atomic charge densities,

$$P_q(z) = 2.5416 \sum_A q_A z_A \quad (\text{Debyes}) \quad (6.36)$$

$$q_A = (Z_A - P_{AA}) \quad (6.37)$$

where A runs over the atoms of the molecule, z_A is the appropriate Cartesian co-ordinate, Z_A is the core charge of the atom, which is the atomic number less two for all atoms except hydrogen since the $1s$ electrons of the heavier atoms are taken to be part of a nonpolarizable core, P_{AA} is the total electronic charge on the atom,

$$P_{AA} = 2 \sum_A \sum_{i \text{ occ}} c_{i\mu}^2 \quad (6.38)$$

where i runs over the occupied orbitals and $c_{i\mu}$ is the coefficient of the μ^{th} atomic orbital in the i^{th} molecular orbital.

The other type is a contribution from atomic polarization resulting from the mixing of the $2s_A$ and $2p_A$ atomic orbitals,

$$p_{sp}(z) = - \sum_{\text{atoms}} P_{2s(A), 2pz(A)} \phi_{2s(A)} \phi_{2pz(A)} d\tau \quad (6.39)$$

$$= -7.3370 \sum_{\text{atoms}} (Z'_A)^{-1} P_{2s(A), 2pz(A)} \quad (\text{Debyes}) \quad (6.40)$$

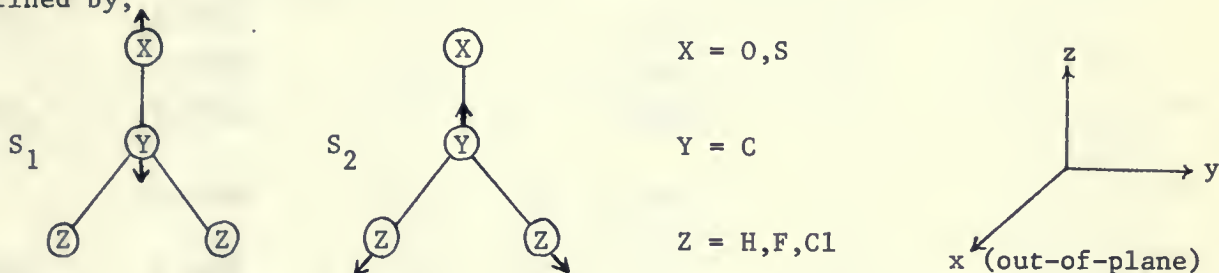
where $P_{2s(A), 2pz(A)}$ is the usual bond order;

$$P_{2s(A), 2pz(A)} = 2 \sum_{i \text{ occ}} c_{i, 2s(A)} c_{i, 2pz(A)} \quad (6.41)$$

and Z'_A is the orbital component of the atom A , taken to be the Slater value.

The dipole moments calculated by the CNDO/2 method of equations (6.36) and (6.40) are generally very bad but are as good as can be expected from other literature reference calculations, including diatomics (28). The molecules investigated were COH_2 , COF_2 , COCl_2 , CSF_2 , CSCl_2 and newly reported CSH_2 . The CNDO/2 computer program calculated the molecular wavefunction and hence the molecular dipole moment at the observed experimental equilibrium geometries as given in Table 6.I. For a particular

molecule a series of calculations was then performed so as to distort the molecular geometry according to the defined symmetry co-ordinates which in effect simulated bond stretching vibrations. For the molecules studied the defined symmetry co-ordinates were either of type S_1 or S_2 defined by,



The bond stretching motions were calculated at intervals ranging from $\pm 0.005\text{\AA}$ to $\pm 0.02\text{\AA}$. The graphs of dipole moment versus bond length were plotted and the derivative obtained by taking the slope at the equilibrium bond length fell near the maximum so that even a slight change in the equilibrium value would cause a gross change in the dipole moment derivative with respect to the symmetrized internal co-ordinate.

The results of the calculations are outlined in Table 6.3. The calculated dipole moment derivatives with respect to internal co-ordinates are generally in good agreement with the magnitudes of the available experimental results. The table gives a brief indication as to the vagueness of the actual sign for the experimental derivatives. The sign ambiguity is very evident from a literature examination of the discussions dealing with experimental data. A physical meaning of the plus and minus sign is very important for the development of trends from the calculated results.

The CNDO theory as outlined by Segal & Klein predicts that there are three basic factors determining the change in dipole moments when simulating a fundamental vibration:

- (a) A change in the sp and pd type polarization of the electrons about the nuclei of the various atoms leads to a net change in the dipole moment.

TABLE 6.3

Molecule	CNDO/2 Equilibrium Geometry	Type of Vibrational Mode	Type of Motion	CNDO/2 Calculated M_j D/° Å	Observed M_j D/° Å
COH ₂	1.253 Å	S ₁	C=O stretch	+3.623	*-1.9 (b)
	1.118 Å	S ₂	C-H symmetric stretch	-0.833	**+1.3 (b)
COF ₂	1.250 Å	S ₁	C=O stretch	+5.714	9.61 ± 0.7 (a)
				or	4.70 ± 0.7
	1.331 Å	S ₂	C-F symmetric stretch	-5.681	3.83 ± 1.9 (a)
				or	5.67 ± 1.6
COCl ₂	1.246 Å	S ₁	C=O stretch	+6.801	7.48 ± 0.2 (a)
				or	4.75 ± 0.2
	1.675 Å	S ₂	C-Cl symmetric stretch	-2.248	2.53 ± 0.36 (a)
				or	3.19 ± 0.36
CSH ₂	1.625 Å	S ₁	C=S stretch	-1.869	
	1.120 Å	S ₂	C-H symmetric stretch	-0.625	
CSF ₂	1.665 Å	S ₁	C=S stretch	+7.500	
	1.326 Å	S ₂	C-F symmetric stretch	-11.400	
CSCl ₂	1.600 Å	S ₁	C=S stretch	-5.977	+3.54 (c)
	1.631 Å	S ₂	C-Cl symmetric stretch	-2.000	-4.21 (c)

* Due to the possible sign combinations the calculated bond moments range from ± 1.20 to ± 3.61 D/° Å

** The calculated values range from ± 0.838 to ± 2.44 D/° Å.

(a) Reference 17

(b) Reference 39

(c) Reference 40

(b) The shift of atoms which bear a net charge in the equilibrium configuration q_A results in a contribution to the dipole.

(c) A change in atomic hybridization on stretching (or bending) modes leads to a net change in the charge upon the component atoms Δq_A with a resultant effect upon the dipole moment

For example, consideration of the data obtained for phosgene (COCl_2) which is typical of the series of molecules studied reveals the following interesting CNDO behaviour. Table 6.4 gives the pertinent calculated data for an S_1 vibration

TABLE 6.4

C=O	{ μ }	Dipole	Calculated		
Bond	Dipole	Moment	Atomic		Binding
<u>Length</u>	<u>Moment (D)</u>	<u>Effects (D)</u>	<u>Charge</u>		<u>Energy(A.U.)</u>
1.174 $\overset{\circ}{\text{A}}$ (exp)	-1.77016	sp +0.46912	O	-0.1400	-1.30372
		pd -2.41560	C	+0.3437	
		<u>densities +0.17631</u>	Cl	-0.1018	
		Total -1.77016	Cl	-0.1018	
1.214 $\overset{\circ}{\text{A}}$	-2.02443	sp +0.45228	O	-0.1493	-1.32071
		pd -2.45103	C	+0.3274	
		<u>densities -0.02568</u>	Cl	-0.0891	
		Total -2.02443	Cl	-0.0891	

For this in-plane stretching vibration the total dipole moment change is calculated to be -0.25429D if the carbon-oxygen bond is lengthened 0.04 $\overset{\circ}{\text{A}}$ in the positive z direction while the other bond lengths and angles are kept constant. The polarization contributions $\Delta\mu_{\text{sp}}$ and $\Delta\mu_{\text{pd}}$ are calculated to be -0.016841 and -0.03543D respectively (Effect (a)). Effect (b) gives a calculated value for the change in densities, $\Delta\mu_q$ of -0.20199 D. The sum of $\Delta\mu_{\text{sp}}$, $\Delta\mu_{\text{pd}}$ and $\Delta\mu_q$ gives a calculated value of -0.25429 D which is the total dipole moment change. The charge on the chlorine atoms is calculated to be -0.1018 in the equilibrium configuration and the charge becomes -0.0891 after the stretching motion, giving rise to an overall change of +0.0127. This value is the result of effect (c) which is relatively small compared with effects (a) and (b). The effect

of this deformation is a net flow of electron density toward the negative end of the molecular dipole. There is also a net polarization of the carbon atom toward the lengthened bond which gives rise to about one quarter of the total dipole change, $\Delta\mu_{sp + pd} = -0.05227D$ as compared to $\Delta\mu = -0.2549D$. Since effects (a) and (b) add, a large value for the dipole moment derivative, is obtained.

In the case of thioformaldehyde, the hydrogens are calculated to bear a net positive charge so that effect (c) is opposed to the net flow of electron density. The change in atomic charge on the hydrogens can be converted to a meaningful unit in Debyes which in turn gives rise to a small value for M_j .

The calculated values for the dipole moment derivative given in Table 6.3 are most encouraging. In the case of $COCl_2$ and COF_2 the agreement between experimental and calculated values is respectable even with the choices available from the experimental work. The formaldehyde calculations do not seem to be consistent with the experimental data which is surprising. The experimental treatment by Hisatsune and Eggers yielded by an intuitive method, a consistent set of derivatives according to sign combinations of the six dipole moment derivatives with respect to normal co-ordinates (39). These workers chose the values $(\partial P/\partial S)_{C=O}$ and $(\partial P/\partial S)_{CH}$ to be -1.9 and $1.3 D/\text{\AA}$ respectively. It is interesting to note that one of their eight sets of solutions gave values for $|\partial P/\partial S|_{C=O}$ and $|\partial P/\partial S|_{CH}$ of 3.48 and $0.838 D/\text{\AA}$ respectively. Our analogous CNDO/2 calculated values were 3.623 and $0.833 D/\text{\AA}$. On this basis it is quite possible that the formaldehyde bond moment derivatives with respect to symmetrized internal co-ordinates have been incorrectly assigned.

Chapter 7

Discussion:

The assignment of the five in-plane fundamental frequencies of vibration for thiocarbonyl chlorobromide has been made. The assignment was achieved by spectroscopic analyses of the solution, liquid and gas phase infrared spectra and the liquid laser Raman spectrum. These spectra are shown in a condensed form in Figure 7.1. Sections A, B and C are the illustrations of gas phase, CS_2 solution phase and liquid phase IR respectively. Sections D and E are the liquid laser Raman spectra with section E at 25 times the relative intensity of section D.

The observed frequencies obtained from the vibrational spectra are listed in Table 7.1. The in-plane fundamental frequencies are assigned at 1130, 764, 438, 257, and 222 cm^{-1} in their proper ν_1 to ν_5 order. The main difficulty in deciding upon a definite assignment was the presence of impurities in the samples analyzed. These impurities were due to the problems encountered in the synthesis and purification of the compound. The two bromination methods that have been successful unfortunately afford very poor yields. These methods involve bromination of the thiocarbonyl dichloride molecule. Better yields could possibly be achieved by solution phase bromination of thiophosgene dimer. Thiocarbonyl fluoride, which is a gas, could also be mono- or dibrominated with anhydrous HBr to yield further molecules in the halide series for spectroscopic study; namely, CSFBr and CSBr_2 . In the future purification procedures will be attempted by gas chromatographic techniques with a closed glass system for collection of the desired product at liquid nitrogen temperature.

The nine Urey-Bradley force constants for CSClBr have been readily transferred and satisfactorily refined. This set for CSClBr has now been added to those previously calculated by our group for the molecules CSF_2 , CSFCl and CSCl_2 . The comparative values for the four thiocarbonyl halide molecules are given in Table 7.2. It must be remembered that the set of force constants which we have

(A) The infrared vapour spectrum of CSClBr at a pressure of 10 mm Hg taken in a 1 metre gas cell with CsI windows.

(B) Same as Figure 4.3

Figure 7.1 (C) Same as Figure 4.4

(D) Same conditions as Figure 4.5

(E) Same conditions as Figure 4.6

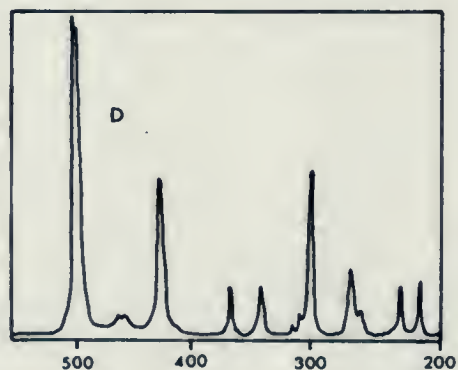
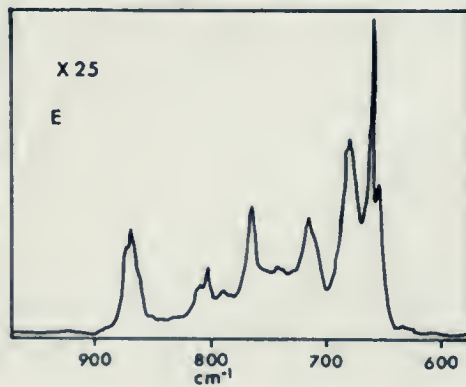
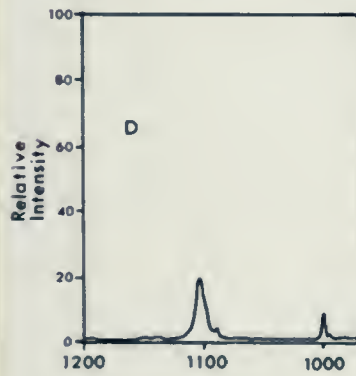
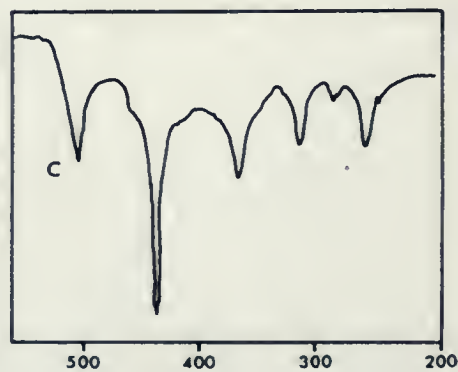
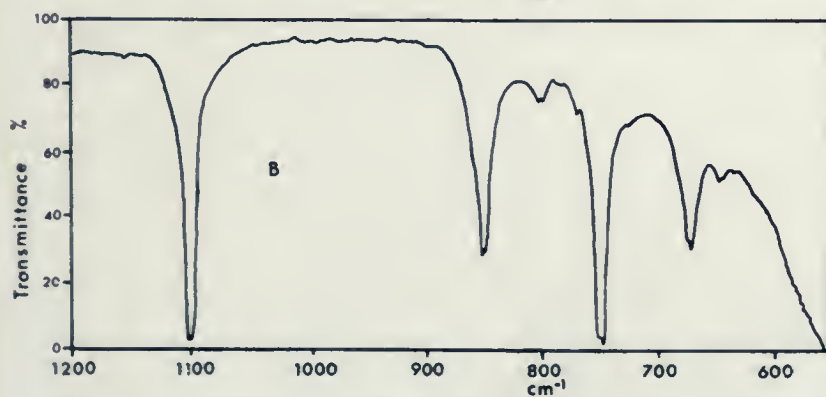
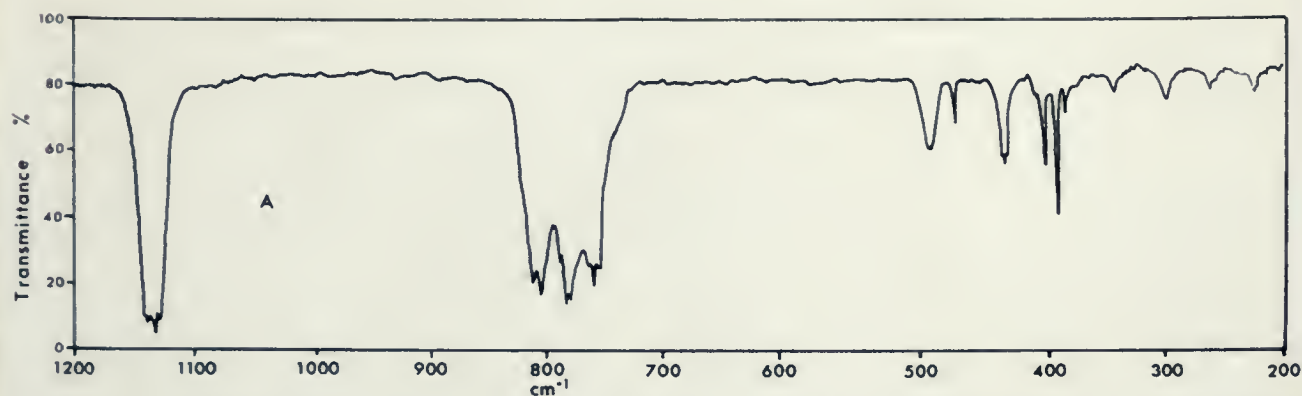


Table 7.1Infrared and Raman Spectra Fundamental Frequencies (cm^{-1})

Fundamental	IR Gas	IR Solution(CS_2)	IR Liquid	Raman Liquid
ν_1	1130	1102		1125
ν_2	764	742		761
ν_3	438		438	437
ν_4	256		256	257
ν_5				222

chosen for CSClBr is only one of the many possible choices. The choice must be taken whenever an attempt is made at calculating force constants from an insufficient number of observed frequencies. However, in light of this difficulty we expect our choice to be the best possible one on the basis of the Urey-Bradley force constant data available for the other thiocarbonyl halide molecules.

The comparison of the Urey-Bradley force constants for the four molecules verifies that the CSCl_2 and CSClBr potential force field environments are very similar relative to those of CSF_2 and CSFCl . On the basis of electronegativities the bromine and chlorine atoms are quite alike while fluorine is very different. The differences in $K_{\text{C=S}}$ for CSCl_2 and CSClBr and K_{CCl} are only 0.2 and 0.9% respectively. The analogous force constant differences between CSCl_2 and CSFCl are 8.2 and 12.1 % respectively. From these results we conclude that a fluorine substituted thiocarbonyl halide molecule has a markedly different Urey-Bradley potential energy force field than a chlorine and/or bromine substituted molecule. This trend also was prevalent in our CNDO/2 calculations on carbonyl and thiocarbonyl halide molecules. Fluorine (COF_2 and CSF_2) calculations led to very strange results in many cases while hydrogen (formaldehyde) and chlorine (COCl_2 and CSCl_2) results were much more reasonable.

The K_{CBr} stretching force constant in CSClBr is 20% larger than in COClBr . K_{CCl} in CSClBr is 17% larger than K_{CCl} in COClBr . These differences are remarkably similar. Also of surprising similarity are the halogen - halogen non-bonded interaction force constants. Although in CSF_2 the F_{FF} force constant value is 1.143 m-dyne / Å, for CSClF , CSCl_2 and CSClBr the values F_{ClF} , F_{ClCl} and F_{ClBr} are 0.761, 0.74 and 0.726 m-dyne / Å respectively. This result is very difficult to explain.

For the molecules studied our CNDO/2 calculated dipole moment derivatives with respect to symmetrized internal co-ordinates were in excellent agreement with available experimental values. From our study we have found that a theoretical determination can be very useful in the interpretation of the complicated solutions for dipole moment derivatives which are the result of experimental

Table 7.2

Urey-Bradley Force Constants
Thiocarbonyl Halides

Force Constant Symbol	m-dyne / Å			
	CSF ₂ ^(a)	CSFCl ^(a)	CSCl ₂ ^(a)	CSClBr
K _{CS}	6.27	5.739	5.327	5.319
K _{CF}	4.483	3.936		
K _{CCl}		2.632	2.352	2.331
K _{CBr}				1.96
H _{FF}	0.425			
H _{C1C1}			0.08	
H _{FC1}		0.321		
H _{C1Br}				0.07
H _{SF}	0.158	0.158		
H _{SC1}		0.101	0.101	0.101
H _{SBr}				0.066
F _{FF}	1.143			
F _{C1C1}			0.74	
F _{C1F}		0.761		
F _{C1Br}				0.726
F _{SF}	0.97	0.97		
F _{SC1}		0.681	0.681	0.681
F _{SBr}				0.55

(a) Reference 12

integrated infrared intensity measurements. We believe, for example, that there is good reason to doubt the chosen values for $(\partial P/\partial S)_{C=O}$ and $(\partial P/\partial S)_{CH}$ in the formaldehyde work of Hisatsune (39). Our Spectroscopy group will be using the theoretical intensity calculations to complement our own experimental intensity measurements on CSF_2 and $CSCl_2$ in the near future.

REFERENCES

1. J. L. Brema, B. Sc. Thesis Brock University (1969)
2. D. C. Moule and C. R. Subramaniam, Chem. Com. 1237, 1340 (1969)
3. D. C. Moule and A. K. Mehra, J. Mol. Spectr. 35, 137 (1970)
4. D. C. Moule, Can. J. Chem. 48, 2623 (1970)
5. D. C. Moule and P. D. Foo, unpublished work
6. H. C. Urey and C. A. Bradley, Phys. Rev. 38, 1969 (1931)
7. J. Overend and J. R. Scherer, J. Chem. Phys. 32, 1289 (1960)
8. G. A. Segal and M. L. Klein, J. Chem. Phys. 47, 4236 (1967)
9. G. W. King "Spectroscopy and Molecular Structure"
Holt, Rinehart and Winston Inc. (1964)
10. M. Davies Editor, J. Overend Author "Infrared Spectroscopy and
Molecular Structure" Chapter X, Elsevier Publishing Co. (1963)
11. B. Crawford Jr., J. Chem. Phys. 29, 1042 (1958)
12. D. C. Moule and C. R. Subramaniam, Can. J. Chem. 47, 1011 (1969)
13. N. Kharasch and C. Y. Meyers "The Chemistry of Organic Sulphur
Compounds" Vol. 2, Chapter 12, Pergamon Press (1966)
14. Handbook of description and instructions, Perkin-Elmer Model 225
Infrared Grating Spectrophotometer, Bodenseewerk Perkin-Elmer & Co.
Ueberlingen, Germany (1967)
15. J. C. D. Brand, J.H. Callomon, D. C. Moule, J. Tyrell and T. H.
Goodwin, Trans. Faraday Soc. 61, 236 (1965)
16. F. Catalano and K. Pitzer, J. Am. Chem. Soc. 80, 1054 (1958)
17. M. J. Hopper, J. W. Russell and J. Overend, J. Chem. Phys. 48, 3765
(1968)
18. J. Overend and J. C. Evans, Trans. Faraday Soc. 55, 1817 (1959)
19. G. Herzberg, "Infrared and Raman Spectra", p216, Van Nostrand,
New York (1945)
20. C. R. Subramaniam M.Sc. Thesis Brock University (1968)
21. K. Shimizu and H. Shingu, Spectrochimica Acta 22, 1528 (1966)
22. B. Schneider and J. Štokr, Collection of Czechoslovak Chemical
Communications 26, 1221 (1961)
23. C. A. Frenzel, K. E. Blick, C. R. Bennett and K. Niedenzu
J. Chem. Phys. 53, 198 (1970)

24. T. Shimanouchi, J. Chem. Phys. 17, 245, 848 (1949)
25. T. Shimanouchi, I. Nakagawa, J. Hiraishi and M. Ishii,
J. Mol. Spectr. 19, 78 (1966)
26. E. B. Wilson Jr., J. C. Decius and P. C. Cross,
"Molecular Vibrations" McGraw-Hill Inc., New York (1955)
27. J. A. Pople, D. P. Santry and G. A. Segal, J. Chem. Phys. 43, S129
(1965)
28. J. A. Pople and G. A. Segal, J. Chem. Phys. 43, S136 (1965)
29. J. A. Pople and G. A. Segal, J. Chem. Phys. 44, 3289 (1966)
30. Quantum Chemistry Program Exchange, Chemistry Department
Indiana University Bloomington, Indiana 47401 (USA)
31. G. A. Segal, J. Chem. Phys. 47, 1876 (1967)
32. K. Takagi and T. Oka, J. Phys. Soc. Japan 18, 1174 (1963)
33. R. H. Jackson, J. Chem. Phys. 77, 2995 (1962)
34. D. W. Robinson, J. Chem. Phys. 21, 1741 (1953)
35. Personal communication, D. R. Johnson, National Bureau of Standards
Washington, D. C.
36. E. B. Wilson Jr. and A. T. Wells, J. Chem. Phys. 14, 578 (1946)
37. S. S. Penner and D. T. Weber, J. Chem. Phys. 19, 807 (1951)
38. G. A. Segal and M. L. Klein, J. Chem. Phys. 47, 4236 (1967)
39. I. C. Histsune and D. F. Eggers, J. Chem. Phys. 23, 487 (1955)
40. R. J. Lovell and E. A. Jones, J. Mol. Spectr. 4, 173 (1960)

REFERENCE

